Linköping University | Department of Electrical Engineering
Master's thesis, 30 ECTS | Electrical Enginering
2023 | LIU-ISY/LITH-EX-A--23/001--SE

Modeling and Control of Fuel Cell Stacks in Autonomous Underwater Vehicles

Modellering och reglering av en bränslecellstack i en autonom ubåt

Simon Andersson

Supervisor : *Max Johansson - ISY, Linköping University*
Examiner : *Lars Eriksson - ISY, Linköping University*

LINKÖPING UNIVERSITY

Linköpings universitet
SE–581 83 Linköping
+46 13 28 10 00 , www.liu.se

Upphovsrätt

Copyright

Abstract

The demand on emission control is increasing every day and is one of the main challenges for propulsion systems. A modern solution is the use of fuel cells which, depending on what kind, can have only heat and water. Fuel cells have become an alternative recently and for underwater vehicles, the upsides of using a fuel cell are many. Autonomous underwater vehicles are used for missions that are dangerous for humans to manually control, for example ocean floor mapping. In order to understand the conditions and limits of the systems inside the submarine a simulation model can be developed and used to emulate a real run of the submarine on the ocean floor. This thesis deals with developing a simulation model that outputs conditions such as temperature and the amount of water inside the chamber with the fuel cell, in order to investigate how the system would behave during real runs.
From the results it can be concluded that it is only if the fuel cell works close to maximum capacity for an extended period of time that overheating in the chamber arises.

Acknowledgments

Firstly, I would express my sincerest gratitude to Max Johansson at Linköping University for taking the role as my supervisor during the project. For always taking the time to help out with his expertise when needed.

I would also like to give a special thanks to my examiner, Lars Eriksson at Linköping University, for kindly offering to let me be a part of this exciting project. An expert with an abundant amount of knowledge within the field.

Linköping, September 2023
Simon Andersson

Contents

List of Figures

List of Tables

1 Introduction

This chapter aims to present an overview of the thesis by introducing the background, purpose and problem formulation of the thesis. It also contains the delimitations of the thesis as well as previous related work.

1.1 Background

Unmanned Underwater Vehicles (UUVs) are for example used for survey missions where sampling of data and mapping of the ocean floor is a few of the interests. There are two sub-classes of UUVs, Remotely Operated underwater Vehicles (ROVs) and Autonomous Underwater Vehicles (AUVs). ROVs are manually controlled and are often tethered to a host ship and is a replacement for humans in difficult underwater conditions. On the contrary, AUVs operates without human input and were developed for collection of data during longer time periods as well as to explore and to map unknown parts of the ocean.

An AUV has been developed for the Swedish Maritime Robotics Centre with two battery packs as its power source. Batteries are the more conventional choice for power but in an effort to increase the range and endurance for the AUV, a potential fuel cell/battery hybrid power system concept has been examined and is to be realised. The investigated solution is to change one of the battery packs to a PEMFC stack.

1.2 Purpose and Goal

The purpose of this thesis is to help make it possible for the group working with the submarine to simulate pre-planned missions. Simulations are a cost-effective and low-risk way of experimenting with and optimizing an application, as long as the model used in the simulation accurately represents the application. Therefore, before sending the AUV out on missions, there is a desire to gain an understanding of the properties and limitations of the application via simulation.

The goal of this thesis work is to develop a model of a pressure chamber containing the fuel cell stack. This model should be able to track, amongst other variables, temperature and pressure in the chamber during a simulation of a mission.
A second goal is to control the valves and compressors in the system. This will require a simple control strategy.
The third goal is to examine the cooling of the fuel cell and conclude if a common cooling solution is adequate for this application.

1.3 Problem Formulation

The main focus of this thesis will be to develop a model of a PEMFC stack active in a pressure chamber in MATLAB/SimuLink. A simplified sketch of the thought to be model is shown in Fig.1.1. The model consist of several components that will have to be modeled, some of witch are the tanks for hydrogen and oxygen, control valves and compressors. The size and pressure of the tanks are fixed in the project and will be modeled corresponding to that. The valves controlling the hydrogen flow to the anode and the oxygen flow to the pressure chambers is to be modeled. For these control valves, the opening and closing of the valve is supposed to be controlled with a simple PID-regulator so the hydrogen mass flow and oxygen level tracks the desired values. The efficiency of the compressors are assumed to be constant while the mass flow through the compressors will be controlled by regulating the speed. The compressors will be modeled to fit the data sheets to the compressors that will be used in the application.

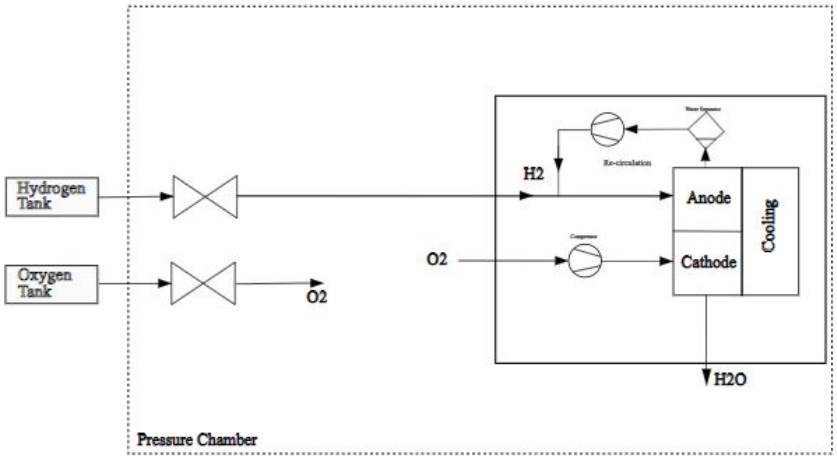

Figure 1.1: Sketch of system

The results of a simulation is the data from the defined outputs of the system. A challenge in this thesis is to handle this data and realize what is interesting to examine more thorough in different scenarios. The outputs that mainly will be considered here are the amount of water as well as the pressure and temperature in the pressure chamber. Furthermore, the pressure in the anode and cathode channel, the fuel cell temperature and the generated power is of interest and will be investigated.

From the description of the problem, the following questions can be formulated:

1. Can the system be modeled to accurately represent the application?
2. Can PID-regulators be used to control hydrogen and oxygen flow?
3. What is the thermal limitations for this application?

1.4 Delimitations

The main focus of this thesis is the modeling of the fuel cell stack inside the pressure chamber. The whole submarine is a hybrid battery/fuel cell system but that will not be taken into consideration, it will be handled as if there were no battery to help with propulsion.
I will not have access to the real application which means that I will not be able to validate the

model by experimentation. So how results vary depending on input will have to be examined and evaluated intuitively.
There is no standard drive cycle for underwater vehicles as there is for road vehicles that can be used. Instead, the current fed to the fuel cell will be adjusted to simulate different scenarios.
Optimization is outside of the scope of this thesis, it mainly considers the modeling of the application and only simple control strategies such as a PID-regulators will be used.

1.5 Related Work

Before being able to work on the modeling, a literature study is conducted and knowledge within the field of the thesis will be obtained.

There are different variants of fuel cells which as varying properties, some examples of different types of fuel cells are High- and Low Temperature Proton-exchange membrane fuel cell (PEMFC) and Solid Oxide Fuel Cells (SOFC). The properties of these different fuel cells are discussed in [12] and an explanation for why Low Temperature PEMFCs are well suited for deep-water applications is given, which also is the conclusion in [1, 13]. Some reasons given by the articles as to why LT-PEMFCs are best suited is that the acoustic signature is low and does not interfere with any sonar readings, as well as the lower thermal signature does not interfere with other sensors on the vehicle. One study showed how different power sources would be better suited for different applications such as for shallow- and deep-water investigations. Furthermore it discusses how depending on the size of the vehicles, what power sources are best suited and which power sources would not be applicable [13].

In [14], a common fuel cell intended for automotive applications is modeled. It provides a good basis for how a fuel cell is modeled, however, as discussed in [4], fuel cells in UUV applications have other challenges than fuel cell powered surface vehicles. The main difference is that for surface vehicles, the oxygen fed to the system can come from the ambient air. Since that is not a possibility underwater, an oxygen storage is needed in the application. Different ways to store oxygen is discussed in this article but the main focus is on the hydrogen storage which gives an insight to the thought process of the storage for the application of this thesis.

According to [8], the reason for the limited progress in implementation of fuel cell power systems in AUVs is because of the complexity and high cost. This in combination with more knowledge in battery power being available explains the reason for commercial AUVs being powered by batteries. A drawback with batteries is that the technology has reached a maturity state, meaning that big improvements in performance is unlikely. In order to increase the range and endurance of an AUV powered by batteries, the size of the AUV would have to increase, which complicates maneuvering. With the current fuel cell technology, an AUV with the same size should be able to have increased range and endurance due to the potentially higher energy density offered by fuel cells [1]. Similar arguments are made in [7] where different types of batteries and a fuel cell system is compared. An in-depth analysis of the challenges for a fuel cell system in an AUV application is made in [6] were possible solutions are presented. An example of a challenge considered is the storage of hydrogen. The hydrogen storage is solved by using 200bar steel tanks. However, this is only proposed as a preliminary solution and using a composite tank would be preferable if it can be developed for high external pressure and seawater.

An important part of operating a fuel cell is to make sure to increase the service life. As discussed in [18], recent studies have shown that an increase in pressure difference between the cathode and anode leads to increased performance. There is, however, a practical limita-

tion to how big the pressure difference can be. A significant pressure difference will damage the membrane and thereby decrease the lifespan of the fuel cell. A solution is to regulate the hydrogen flow to the anode by controlling a valve between the hydrogen tank and the anode.

The procedure of starting up and shutting down a fuel cell is important to do right in a real life application. [15] is a patent on how to safely start a fuel cell and to keep it in good condition, avoid corrosion causing performance degradation. It describes how the re-circulation in the anode, which could be filled with oxygen, first should be initiated and have a limited flow of hydrogen containing fuel. In this recycle loop, a catalyst is used for the hydrogen and oxygen to react and to form water. The hydrogen flow should be regulated so the mixture of oxygen and hydrogen do not produce a flammable ratio. This goes on until substantially no oxygen is left in the loop and normal hydrogen fuel operating flow rate can gradually be obtained.
In [16], which is a patent for how to shut down a fuel cell, it is explained how stopping the fuel flow and displacing the hydrogen with oxygen quickly improves the long-term performance of the fuel cell.
These two patents show how their proposal minimizes fuel cell degradation without the need for external gases to fill the fuel cell during rest as previous solutions.

2 Theory

In this chapter, the theory that is used in this thesis is presented.

2.1 Fuel Cell

A fuel cell is a device that produces electricity by converting chemical energy through an electrochemical reaction. For fuel cells with hydrogen as the fuel, the products of the reaction is water and heat, unlike an ICE which emits carbon dioxide among other emission. Also unlike an ICE which first converts fuel energy to thermal energy to then convert to mechanical energy, a fuel cell converts fuel energy directly to electrical energy. Therefore, it is not limited by the Carnot Cycle [17].

A similarity that the fuel cells shares with batteries is that batteries also converts fuel energy directly to electrical energy. However, the reactants in a fuel cell is stored externally while in a battery it is stored internally.
As mentioned, fuel cells are not limited by the Carnot Cycle. There is however some heat generated from the reactions that warrants cooling too keep the fuel cell temperature in a favourable range. Because of the heat loss, a fuel cell generally has an efficiency of around 40-60%. The explanations and derivations from James Larminie and Andrew Dicks in [11] leads to the following equation to calculate the efficiency

$$\text{Efficiency}, \eta = \mu_f \frac{V_c}{E_{HHV}} \tag{2.1}$$

where μ_f is the ratio of amount of input fuel and the amount of fuel reacted, which is estimated to 0.95. V_c is the voltage output from a single cell. E_{HHV} is the cell voltage that would be obtained in a 100% efficient system and comes from the equation

$$E_{HHV} = \frac{-\Delta\bar{h}_f}{2F} \tag{2.2}$$

where $\Delta\bar{h}_f$ is the reaction enthalpy and is equal to -285.84 kJ mol^{-1} for the Higher Heating Value. F is the Faraday constant and is equal to 96485 C mol^{-1}.

In general a fuel cell works by feeding fuel to an electrode, called the anode, where an oxidation reaction occurs and the fuel separates into ions and electrons.
In this thesis, a Low Temperature-Proton Exchange Membrane Fuel Cell (LT-PEMFC) is used. In a LT-PEMFC, the fuel is hydrogen gas which means that the reaction results in protons

and electrons.

$$2H_2 \rightarrow 4H^+ + 4e^- \tag{2.3}$$

The electrons flow through an external circuit producing electricity. This circuit goes to the other electrode, called the cathode.
Between the anode and cathode is the Membrane Electrode Assembly, (MEA). It consist of a Polymer Electrolyte Membrane, a catalyst layer on both the anode and cathode side, as well as a gas diffusion layer on both sides. The most commonly used Polymer Electrolyte Membrane in a PEMFC is Nafion. The electrolyte needs to be able to conduct hydrogen ions as well as be electrically insulated so the protons from the anode can pass through while the electrons is forced through the external circuit. It is also helpful if the electrolyte is stable both thermally and chemically.
Apart from the electrons and the protons from the anode reaching the cathode, oxygen is supplied to the cathode and a reduction reaction occurs. The reaction is between protons, electrons and oxygen and results in water.

$$O_2 + 4H^+ + 4e^- \rightarrow 2H_2O \tag{2.4}$$

Giving the overall reaction

$$2H_2 + O_2 \rightarrow 2H_2O \tag{2.5}$$

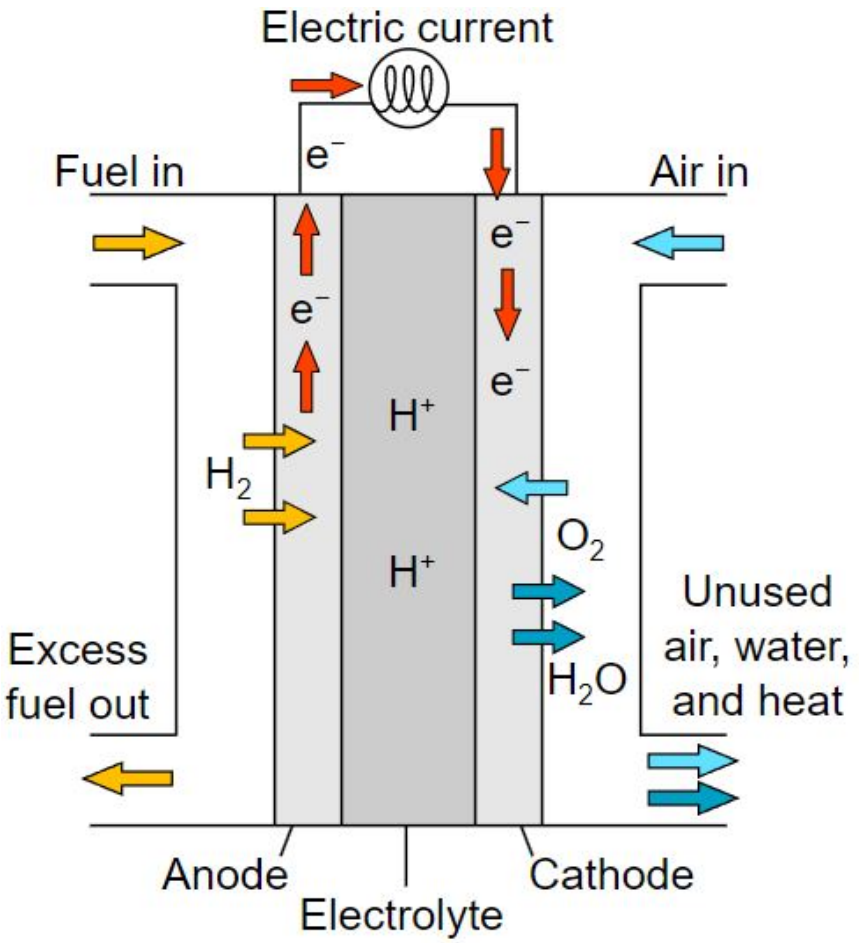

Figure 2.1: Reaction in a fuel cell [10]

Depending on operation conditions, one cell produces a voltage of between 0-1 volts. Typically, the fuel cell voltage is somewhere around 0.7 volts [2]. To increase the total fuel cell voltage output, the cells is stacked in series, named a fuel cell stack. This is what allows a fuel cell to produce enough voltage to be able to be used, for example, in submarines.

2.2 Fuel Cells in Underwater Vehicles

How to power a submarine have always been a difficult task. One historically common way is to use diesel engines in combination with batteries to power the propellers. The diesel engine charges the batteries so they can power the propulsion system during dives. However, since batteries can only hold so much power, the submarines can not stay under water for too long and has to surface in order to obtain air for the diesel engines to charge the batteries again. A submarine does not have to fully surface, it can cruise close to surface and use snorkels to get fresh air to power the diesel engines.

Another solution is to use a nuclear reactor to power the submarine. A nuclear submarine is not dependent on air and therefore does not have to resurface as often as the diesel-electric submarine. The heat from the nuclear reaction is used to generate steam that drives a steam turbine. The turbine powers the propellers and electrical generators for auxiliary devices in the submarine.

For smaller submarines, such as the one considered in this thesis, using a nuclear reactor is to expensive and complex. Using a diesel-electric solution is not optimal since there are emissions having a negative impact on the environment. The most common solution for smaller submarines is to only use batteries. Since the power required to drive a smaller submarine is less, it is possible to use batteries and obtain dives with long range. However, the research in the field of batteries has reached a maturity state and big improvements is unlikely to occur [1]. Of fuel cells on the other hand, there is not as much knowledge but it is already contending with batteries for use in low to zero emissions propulsion systems. Fuel cells have a greater power density than batteries and therefore it is possible to obtain more power from less weight.

For smaller submarines, using fuel cells to power the propulsion system is appropriate. Unlike for the diesel-electric solution, depending on what type of fuel cell that is used, there is zero or close to zero emissions. Compared to the nuclear reactor solution, it is much less expensive and complex. The nuclear reactor also produces a lot of heat and noise which can disrupt sonars and sensors that could be of use for the submarine. Compared to batteries the main upside is the superior power density.

Using a fuel cell does not come without challenges. There have been limited research on fuel cell so there are still a big cost in development to optimize the use of fuel cells. The hydrogen needs to be stored and these storage solutions are complex and expensive. Hydrogen is also highly flammable and could cause explosions if not handled correctly. A specific problem to fuel cell in submarines is the working conditions for the fuel cell. Ambient temperature affects how effective the fuel cell is but it can operate with an ambient temperature between -10 to 70 degrees Celsius. The problem is that the ambient pressure needs to be somewhere between 0.7 to 1.5 bar. During dives with submarines, the pressure quickly exceeds 1.4 bar, therefore a pressure chamber is necessary to use.

2.3 Fuel Cell Cooling

As mentioned, the fuel cell generates heat that needs to be dissipated in order to maintain a favourable operating temperature. A good operating temperature for LT-PEMFCs is around 80 degrees Celsius. There are several cooling methods including, for example, cooling with separate airflow and the use of a coolant loop. For fuel cells producing power less than 2 kW, a separate airflow should be enough [19]. The fuel cell that is used in this thesis produces a maximum of 1 kW and so a separate airflow is enough. However, it is an autonomous submarine that will be out of reach for long periods of time. Therefore redundancy is important and a coolant loop should be used.

Coolant Loop

A coolant loop uses a cooling liquid that has a high thermal conductivity and heat capacity. This means that the liquid is effective at transferring heat from the fuel cell to the liquid as well as dissipate it to the ambient air. A simple coolant loop is shown in Fig.2.2.
Cooled liquid is pumped to the fuel cell where it transfers heat from it. Thereafter it passes through a three-way valve that either sends the liquid directly back the pump or trough a radiator. This valve is controlled using the temperature of the fuel cell. If the working fuel cell temperature is equal or lower than desired, the liquid is directly fed to the pump. If the working temperature of the fuel cell is higher than desired, the liquid is fed trough the radiator to cool. The radiator works by having channels that the liquid goes trough while

fans blow ambient air on it. This results in cooling of the liquid and heating of the ambient air.

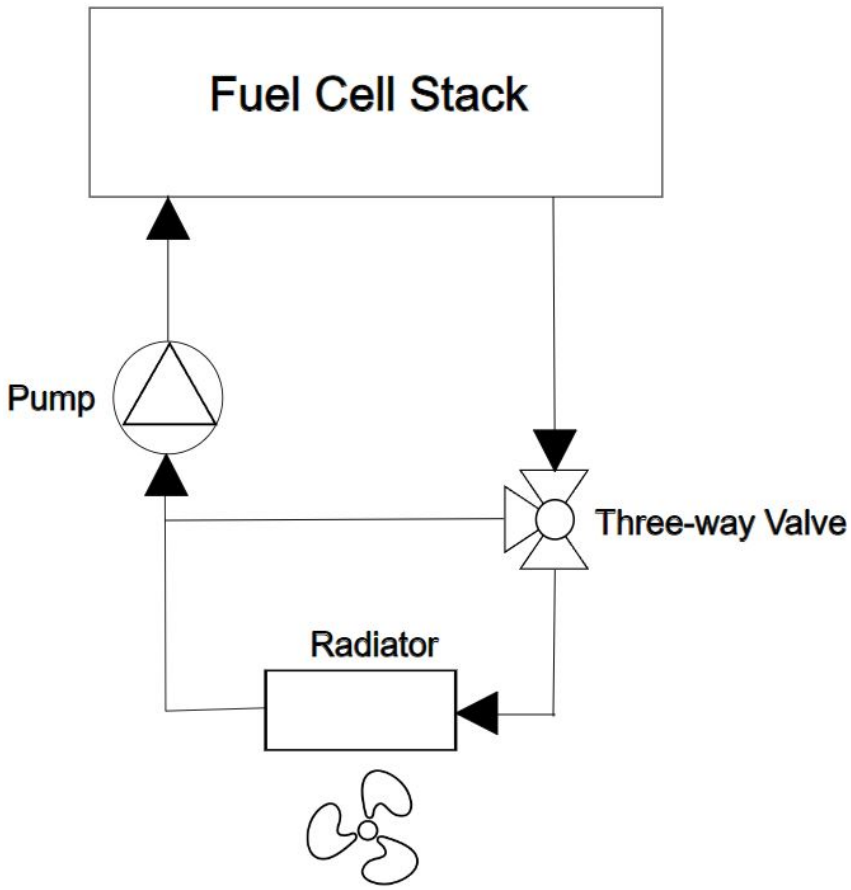

Figure 2.2: Cooling solution using simple coolant loop

Temperature in the Pressure Chamber

Table 2.1: Constants and variables for chamber temperature

Constants and Variables	**Values and Units**
Chamber area, A	1.2 [m]
Thermal conductivity air, k	0.03 [w/mK]
Gravitational acceleration, g	9.81 [m/s^2]
Chamber diameter, D	0.43 [m]
Coefficient of thermal expansion air, c	$3.4e^{-3}$ [$10^{-}6/°C$]
Specific heat capacity air, Cp	1004 [J/kgK]
Dynamic viscosity air, μ	$1.8e^{-5}$ [kg/ms]
Temperature outside chamber, T_a	277 [K]
Universal gas constant, R	8.314 [J/(mol K)]
Molecular mass, M_j $(H_2, O_2, H_2O, N2)$	0.002,0.032,0.018,0.028 [kg/mol]
Kinematic viscosity, v	[m^2/s]
Thermal diffusivity, α	[Ns/m]
Prandtl number, Pr	[-]
Rayleigh number, Ra_D	[-]
Nusselt number, Nu	[-]
Average heat transfer, h	[W/m^2K]
Heat loss from chamber, q_c	[W]
Temperature inside chamber, T_c	[K]
Heat transfer from fuel cell cooling, Q	[W]
Partial pressures, p_j $(H_2, O_2, H_2O, N2)$	[Pa]

The temperature in the pressure chamber increases from the cooling of the fuel cell. Since the temperature of the ambient air can not exceed a certain point in order for the fuel cell to work, the temperature has to decrease in some way. Since the submarine, during fuel cell operation, dives deep in the ocean, the ambient temperature of the chamber is around 4 degrees Celsius. Natural convection will occur and the chamber will transfer heat to the surrounding water and the temperature in the chamber can be calculated. The chamber is a cylinder and natural convection for a horizontal cylinder gives the calculations below and the variables and constants are given in Table 2.1.
Heat loss from the chamber

$$q_c = h * A * (T_c - T_a) \tag{2.6}$$

To calculate the total heat transfer for the chamber, the heat transfer from the cooling of the fuel cell, Q, is subtracted by the heat loss from the chamber, q_c

$$\Delta q = Q - q_c \tag{2.7}$$

The temperature in the chamber is then calculated by integrating the product of the following equation

$$\frac{dT_c}{dt} = \frac{\Delta q}{\rho C_p V} \tag{2.8}$$

where ρ is calculated by

$$\rho = \frac{\sum M_j * p_j}{RT_c} \tag{2.9}$$

M_j is the molar mass for four different molecules; hydrogen, oxygen, water and nitrogen. p_j is the partial pressures of hydrogen, oxygen, water and nitrogen.
The average heat transfer coefficient is a proportionality constant between heat flux and temperature difference and is calculated as

$$h = Nu * \frac{k}{D} \tag{2.10}$$

For natrual convection with external flow over a horizontal cylinder, which most accurately describes a simplified model of the chamber, the Nusselt number is calculated according to [3] in the following equation

$$Nu = \left(0.6 + \frac{0.387 * Ra_D^{1/6}}{\left(1 + \frac{0.559}{Pr}^{9/16}\right)^{8/27}}\right)^2 \tag{2.11}$$

To calculate the Nusselt number, the Rayleigh, which describes the relationship between bouyancy and viscosity within a fluid, and the Prandtl number, which is defined as the ration between the momentum and thermal diffusivity, is needed [3]

$$Ra_D = g * c * (T_c - T_a)\frac{D^3}{\alpha * v} \tag{2.12}$$

$$Pr = v/\alpha \tag{2.13}$$

To calculate the Prandtl number, momentum diffusivity (α) and thermal diffusivity (v) is needed

$$\alpha = \frac{k}{\rho * Cp} \tag{2.14}$$

$$v = \frac{\mu}{\rho} \tag{2.15}$$

3 Method

This chapter contains the method used to carry out the work in this thesis.

3.1 Modeling

Modeling a fuel cell inside a pressure chamber is the main focus of this thesis and the work is carried out in MATLAB/SimuLink. The fuel cell will be modeled according to Pukrushpan's work in [14]. The inputs to the fuel cell is hydrogen flow, air flow and a current.
The hydrogen flow comes from a pressurized hydrogen tank located outside the chamber and between the anode side of the fuel cell and tank there is a valve that controls the mass flow of the hydrogen to be in favourable working condition for the fuel cell. There is also a re-circulation system that contains a hydrogen blower and a catalytic afterburner so unused hydrogen is disposed safely. The afterburner has more practical importance but the re-circulation should be modeled to imitate the real application.

On the cathode side there is a compressor that takes the ambient air to the cathode and is controlled so the mass flow of the air gives the desired cathode pressure. Since the fuel cell uses oxygen as a reactant there is a constant decreasing value of oxygen in the chamber during work. Therefore a pressurized oxygen tank is located outside the chamber and provides oxygen to the chamber via a valve controlling the amount of oxygen fed to the chamber.

The current demand from the fuel cell affects the resulting power output from the fuel cell. The current will be manipulated so the power produced from the fuel cell will emulate interesting test cases. For example, the fuel cell that will be used is rated for 1 kW, if the fuel cell is close to providing maximum power for an extended period of time, it is of interest to know how it will affect the conditions in the chamber.

As mentioned there should be a pressure difference between the anode and cathode, how big the pressure difference should be is dependent on the fuel cell. In the case of this thesis, the pressure difference is arbitrarily chosen to be 3kPa higher in the anode. To control this pressure difference in a simple and effective way, a PID-regulator controlling the valve is used.

Fuel Cell Stack

There are many books and papers written on how to model a fuel cell. Jay T. Pukrushpan is well regarded in this field and provides a model in [14] that, as mentioned, will be used in this thesis. Not all of the chemical energy is converted to electrical energy in a fuel cell reaction. There are also some conversion to heat, as well as three other types of losses that will be discussed.

Open Circuit Voltage

The Gibbs free energy represents the available energy to do external work and the change in Gibbs free energy, Δg_f, is

$$\Delta g_f = g_f \text{ of products } - g_f \text{ of reactants} \tag{3.1}$$

The chemical reaction for a fuel cell using hydrogen is

$$H_2 + \frac{1}{2}O_2 \rightarrow H_2O \tag{3.2}$$

This leads to the change in Gibbs energy

$$\Delta g_f = (g_f)_{H_2O} - (g_f)_{H_2} - (g_f)_{O_2} \tag{3.3}$$

In [2] it is shown that the Gibbs free energy varies with temperature and pressure according to

$$\Delta g_f = \Delta g_f^0 - RT_{fc}\ln\left(\frac{p_{H_2}p_{O_2}^{1/2}}{p_{H_2O}}\right) \tag{3.4}$$

R is the universal gas constant and the partial pressures for hydrogen, oxygen and vapor (p_{H_2}, p_{O_2} and p_{H_2O}) is expressed in Bar. Δg_f^0 is the change in Gibbs free energy at 1 Bar. T_{fc} is expressed in Kelvin and how Δg_f^0 varies with some different temperatures is given in Table. 3.1.

Table 3.1: Different temperatures effect on change in Gibbs free energy [14]

Temperature [°C]	Δg_f^0 [kJ/mol]
25	-237.2
80	-228.2
100	-225.2
200	-220.4
400	-210.3

The value of the change in Gibbs free energy is negative which means that energy is released from the reaction.
In an ideal process, all chemical energy would convert to electrical energy. Electrical energy is the electrical work used to move electrical charge around a circuit, expressed in Joules and calculated as

$$\text{Electrical work done} = -2FE = \Delta g_f \tag{3.5}$$

From one mole of hydrogen there are two moles of electrons that passes through the external

circuit. The Faraday constant F is the electric charge of one mole electrons and E is the voltage of the fuel cell.

Equation (3.5) coupled with equation (3.4) gives the equation for the reversible voltage

$$E = \frac{-\Delta g_f^0}{2F} + \frac{RT_{fc}}{2F}\ln\left(\frac{p_{H_2}p_{O_2}^{1/2}}{p_{H_2O}}\right) \tag{3.6}$$

The voltage in equation (3.6) is called the reversible open circuit voltage or Nernst voltage of a hydrogen fuel cell. In practice however, the fuel cell process is not reversible and the fuel cell voltage is less than whats given in equation 3.6.
Using standard state, where the temperature is 25°C and the pressure is 1 atm, $\frac{-\Delta g_f^0}{2F}$ has a reference potential of 1.229V. This varies with the temperature and is calculated by

$$\frac{-\Delta g_f^0}{2F} = 1.229 + (T_{fc} - T_0)\left(\frac{\Delta S^0}{2F}\right) \tag{3.7}$$

where T_0 is the temperature in the standard state, 25 °C or 298.15 K and ΔS^0 is the change in entropy. The change is entropy in a given reaction with minimal change in temperature can be considered constant and using equations (3.6) with (3.7) together with this and the constants expressed in their values results in

$$E = 1.229 - 0.85 * 10^{-3}(T_{fc} - 298.15) + 4.3085 * 10^{-5}T_{fc}\left(\ln(p_{H_2}) + \frac{1}{2}\ln(p_{O_2})\right) \tag{3.8}$$

The pressures, p_{H_2} and p_{O_2}, is expressed in atm.

Activation Loss

First of the three main losses in a fuel cell operation is the activation loss, also called activation overvoltage. There is an activation barrier that impedes the conversion of reactants to products and a portion of the fuel cell voltage is used to overcome this barrier. Electrochemical reactions occurs at interfaces and produced current is proportional to the area of the interface. Therefore current density (current per unit area) is used to compare the reactivity of different surfaces.

The activation loss is approximated by

$$\eta_{act} = v_0 + v_a(1 - e^{-c_1 i}) \tag{3.9}$$

where i is the current density. v_0 is the voltage drop at zero current density, v_a and c_1 are fuel cell dependent constants.
In figure 3.1 the voltage drop calculated from equation 3.9 with arbitrary constants is shown.

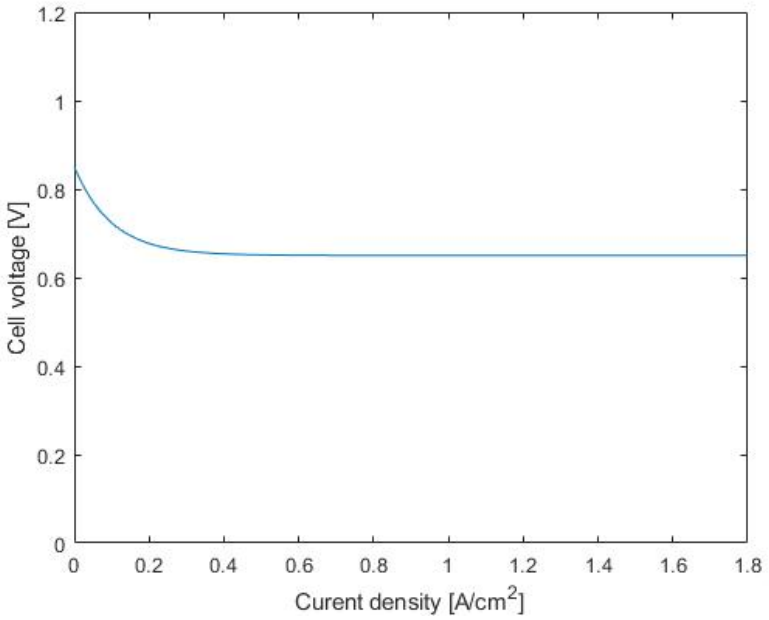

Figure 3.1: Voltage drop due to activation loss

Ohmic Loss

The second loss is the ohmic loss. It is the resistance from the membrane to transfer the protons from the anode to the cathode and the resistance of the electrode to transfer electrons. The voltage drop is proportional to the current density and is described by

$$\eta_{ohm} = i * R_{ohm} \tag{3.10}$$

where R_{ohm} is the internal electrical resistance and has the unit Ωcm^2. This internal electrical resistance is calculated by

$$R_{ohm} = \frac{t_m}{\sigma_m} \tag{3.11}$$

where t_m is the membrane thickness and σ_m is the membrane conductivity $(\Omega\text{cm})^{-1}$. The membrane conductivity is in turn modeled as a function of the membrane water content, λ_m, the fuel cell temperature and model parameters.

$$\sigma_m = (b_{11}\lambda_m - b_{12})\exp\left(b_2\left(\frac{1}{303} - \frac{1}{T_{fc}}\right)\right) \tag{3.12}$$

The constants are usually determined empirically.
In figure 3.2 the voltage drop calculated from equation 3.10 using arbitrary constants is shown.

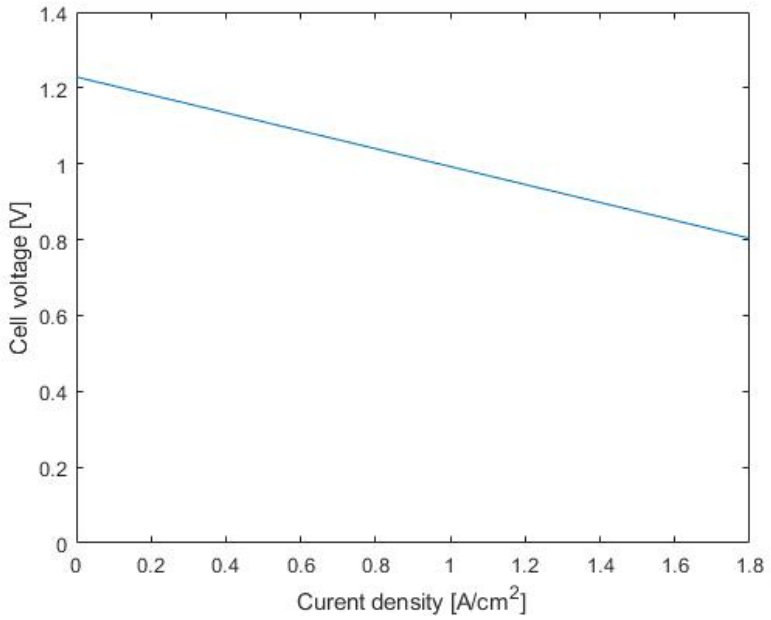

Figure 3.2: Voltage drop due to ohmic loss

Concentration Loss

The last loss is the concentration loss. This loss occurs at high current density and is the result of losses due to mass transport, fuel or oxygen is used faster than supplied. An approximation of the loss is described by

$$\eta_{conc} = i\left(c_2 \frac{i}{i_{max}}\right)^{c_3} \tag{3.13}$$

where i_{max} is the current density for which a very steep voltage drop occurs. c_2, c_3 and i_{max} is determined empirically.
In figure 3.3 the voltage drop calculated from equation 3.13 using constants from the work of Pukrushpan [14] is shown.

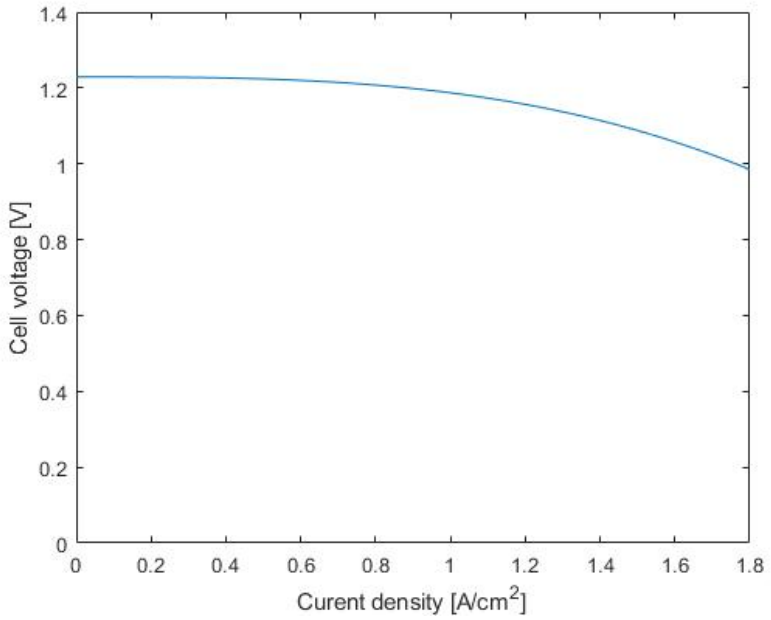

Figure 3.3: Voltage drop due to concentration loss

These losses combine for a total voltage drop over current density, the equation is shown in 3.14 and the result is shown in figure 3.4.

$$V = E - \eta_{act} - \eta_{ohm} - \eta_{conc} \tag{3.14}$$

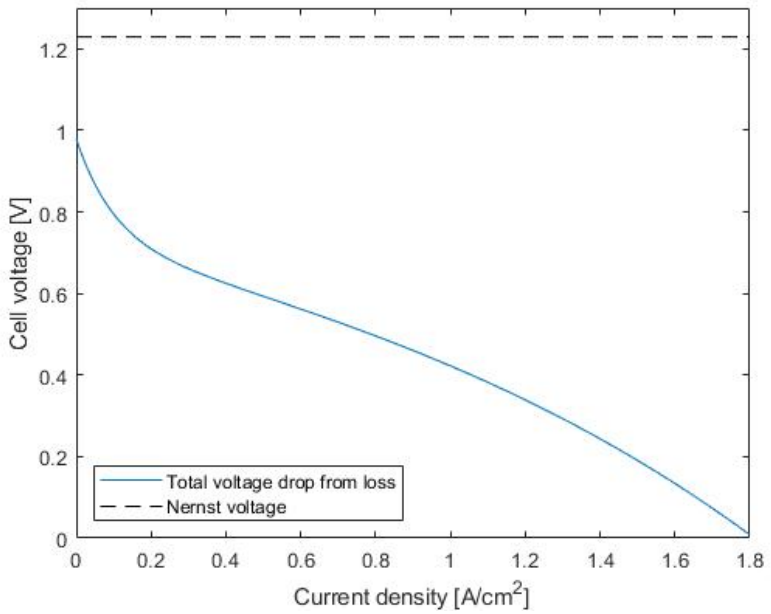

Figure 3.4: Voltage drop due to total loss

Fuel Flow

The fuel flow contains three main subsystem. The anode flow, the re-circulation flow and the flow from the tank to the anode. The anode flow model comes from Pukrushpans work in

[14]. The pressure in the anode is of interest and in order to calculate that, the mass flows over the anode is needed. The states of hydrogen mass and water mass inside the anode volume is calculated by

$$\frac{dm_{H_2,an}}{dt} = W_{H_2,an,in} - W_{H_2,an,out} - W_{H_2,reacted} \tag{3.15}$$

$$\frac{dm_{w,an}}{dt} = W_{v,an,in} - W_{v,an,out} - W_{v,membrane} \tag{3.16}$$

where W is the mass flow rate in kg/sec denoted by either hydrogen, water or water-vapor entering or leaving the anode.
Using this, the partial pressures in the anode can be calculated which adds up to the anode pressure. The partial pressures are calculated by using the ideal gas law

$$p_{j,an} = \frac{m_{j,an} R_j T_{fc}}{V_{an}} \tag{3.17}$$

where j is either hydrogen (H_2) or water-vapor (v). Using this the anode pressure can be expressed as

$$p_{an} = \sum p_{j,an} = p_{H_2,an} + p_{v,an} \tag{3.18}$$

The mass flow in to the anode comes partly from the re-circulation but mainly from the tank. The hydrogen tank which will be used has a volume of 10 litres and the hydrogen will be compressed to 200 Bar. The hydrogen flow from the tank is controlled by calculating the reaction flow in the anode and adjusting for the pressure difference by the actual pressure in the anode and the reference pressure. In this case the reference pressure is fairly arbitrary and can be set high since there will be a valve controlling the flow between the tank and the anode. The valve is controlled by the pressure difference in the cathode and anode. As mentioned in the previous chapter, the pressure in the anode should be slightly higher than the pressure in the cathode. The valve is therefore controlled to regulate the hydrogen flow to the anode to keep the pressure difference constant.

The model of the re-circulation is the mass flow leaving the anode re-circling to enter the anode again. Between this there is a separator where the collected vapor leaves the system, a purge with a catalytic afterburner where unwanted oxygen can react with hydrogen and leave the system, and a hydrogen blower. The catalytic afterburner is of use in the practical system since there can be oxygen in the anode which can hurt the fuel cell.

The pump is modeled empirically using a data sheet from the pump that will be used in the real application. From the data sheet, values of the flow for different pressures and speeds are extracted and put into Matlab where a polynomial fit is done. The pump is controlled by regulating the speed to keep a constant pressure difference between the anode and cathode.

Air Flow

The air flow consists of two main subsystems. The cathode flow and the flow in the chamber. Again, the cathode flow model comes from Pukrushpans work in [14] and is similar to the anode flow model. The states of oxygen mass, nitrogen mass and water mass inside the

cathode model is calculated by

$$\frac{dm_{O_2,ca}}{dt} = W_{O_2,ca,in} - W_{O_2,ca,out} - W_{O_2,reacted} \tag{3.19}$$

$$\frac{dm_{N_2,ca}}{dt} = W_{N_2,ca,in} - W_{N_2,ca,out} \tag{3.20}$$

$$\frac{dm_{w,ca}}{dt} = W_{v,ca,in} - W_{v,ca,out} - W_{v,ca,gen} \tag{3.21}$$

In order to get sufficiently much oxygen to the cathode there is a compressor that feed ambient air to it. The compressor is controlled by minimizing the difference between the reference air flow and the measured air flow. The reference oxygen flow is calculated from the given current and the electrochemical reaction.

Since oxygen is the only reactant in the reaction from air, the flow from cathode to the chamber contains air with reduced oxygen, and water vapor. In order to keep the pressure in the chamber at around 1 atm and also fill up the chamber with oxygen, an external tank of oxygen is used. The tank has a volume of 10 litres and the oxygen is compressed to 200 Bar. From the tank the oxygen goes trough a valve. The valve is controlled to regulate the difference in the measured partial pressure of oxygen inside the chamber compared to the reference partial pressure of oxygen in standard ambient air. The volume of the chamber when empty is estimated to be 0.54 m^3 or 540 litres. Since the chamber will have the fuel cell, cooling system as well as tubes and valves it is assumed that only 20% of the volume will consist of air. This gives the chamber a volume of 108 litres.

Thermal Management

In the thermal management subsystem, the temperature of the fuel cell is calculated. The heat transfer between the fuel cell, coolant liquid and the air in the chamber is also modeled. The calculation of the fuel cell temperature is the integration of the following equation

$$\frac{dT_{fc}}{dt} = \frac{Q_{fc} - Q_{cool}}{m * Cp} \tag{3.22}$$

where Q_{fc} [W] is the heat generation from the fuel cell, Q_{cool} [W] is the heat transfer to the cooling liquid and m [kg] and Cp [J/kgK] is the mass and specific heat capacity of the fuel cell respectively.
This is similar to the heat transfer for air discussed in the previous chapter. However, the coolant flows trough tubes and changes some calculations. In [9], Holman shows that

$$Q_{cool} = W * Cp * (T_2 - T_1) \tag{3.23}$$

where W (kg/s) is the mass flow of the coolant, Cp is the heat capacity of the coolant and T_1 and T_2 is the outlet and inlet temperature of the coolant to the fuel cell respectively. The

outlet temperature is calculated as

$$T_2 = \frac{a_2 * T_f c + (a_1 - a_2/2)T_1}{c_1 + c_2/2} \tag{3.24}$$

$$c_1 = WCp \tag{3.25}$$

$$c_2 = h\pi dL \tag{3.26}$$

where h is calculated the same way as in equation 2.10 but the Nusselt number is different for this case and is expressed as

$$Nu = 3.66 + \frac{0.0668\frac{d}{L}RePr}{1 + 0.04(\max(\frac{d}{L}RePr, 1e^{-10}))^{2/3}} \tag{3.27}$$

where Pr is shown in equation 2.13, d (m) is the diameter of the tube and L (m) is the length off the tube. Reynolds number is

$$Re = \frac{\rho v d}{\mu} \tag{3.28}$$

where ρ is the density of the coolant, v is the velocity of the coolant and μ is the dynamic viscosity of the coolant. The velocity of the coolant is calculated as

$$v = \frac{W}{\rho A} \tag{3.29}$$

where A (m^2) is the area of the tube.

The three-way valve is controlled by the difference between the reference fuel cell temperature and the measured fuel cell temperature where the reference temperature is 80°C. The pump is modeled as a tank which gives a constant flow off coolant from it. The radiator model has surrounding temperature, pressure and mass flow of air as well as inlet temperature, pressure and mass flow of the coolant as the inputs. The output is again the temperature, pressure and mass flow of the air, together with the temperature, pressure and mass flow of the coolant and the heat transfer.

3.2 Simulations

The simulations in SimuLink will provide a good understanding of the conditions in the chamber off the real submarine during work. The power output of the fuel cell is mainly controlled by the input current which will be set to emulate certain work scenarios. Since there is not a velocity standard for submarines as there are for road vehicles, the fuel cell power output is arbitrarily set for different scenarios. It is important to simulate close to maximal power output from the fuel cell since this is the extreme case. However, a more realistic power output is lower since that puts less strain on the fuel cell.

One scenario is to use close to full power output from the fuel cell for a long duration. This is unlikely to be needed in real runs but the steady state conditions in the chamber for maximum output is of interest.

A second scenario of interest is a run with low power output for a long duration. This will give an understanding of the system and the conditions in the chamber during less demanding runs.

Another scenario of interest is pulsating power with peaks that produce close to full power and with lows that produce more reasonable power. How the system and chamber condition reacts to pulsating current is important to understand since it is likely that the submarine needs fluctuating power outputs during runs.

It is also beneficial to simulate a long run with realistic power output. This will give an understanding of how the system works and how the conditions in the chamber will typically be during runs. A realistic power output is difficult to define but it is likely that the power output only needs to rise for short periods at a time, the rest of the time it should be enough with a low power output. It is also convenient to not have to start and stop the fuel cell so for the majority of the time during run, the power output should be low as to not wear down the fuel cell to much.

Another scenario is a simulation where the fuel cell does not output any power for a long period of time after a short low power output will be simulated to understand the conditions inside the chamber in the scenario where power from the fuel cell is not needed.

To emulate a start of the fuel cell the initial condition in the anode is set to be air. For the first part of the simulation, the anode is depleted of air by gradually lowering the partial pressures of its components. At the same time as this procedure, the hydrogen fuel is introduced to the anode which causes the fuel cell voltage to increase. The next step is to connect a current which in turn will lower the voltage produced but also produce a power.
The shutdown procedure is emulated by gradually decreasing the partial pressure of hydrogen and increasing the partial pressure of air components, as well as lowering or disconnecting the current. A lower current leads to a bigger voltage while replacing hydrogen with air decreases the voltage.
The decrease in voltage when there is only a small amount of hydrogen is explained by equation 3.8. A partial pressure of hydrogen going towards zero would cause the last part of the equation to go toward negative infinity, thus giving a total voltage of negative infinity. Since this is not possible, the partial pressure of hydrogen inside the anode is modeled to be bigger than zero. In case of a very small hydrogen partial pressure,the voltage could theoretically obtain a negative value, this is not physically feasible so the voltage is modeled to not be negative. Another voltage that can not be negative is the resulting voltage in equation 3.14 which is also modeled to not be negative.
The voltage graph in [20] is used as a reference when tuning the model to mimic a realistic start and stop cycle. In order to obtain a similar graph a term has been added to the concentration losses from Pukrushpans work that increases with lower partial pressure of hydrogen in the anode.

4 Results

This chapter contains the results obtained from the simulations.

4.1 Simulations

The result from different simulation runs is presented below. The scenarios are the ones discussed previously, a constantly high power output, a constantly low power output, a pulsating high power output, a realistic power output run and a no power output run.

Run With High Power Output

For a run with high power output, the demanded current is set to 50A which results in the power output shown in figure 4.1 and 4.2.

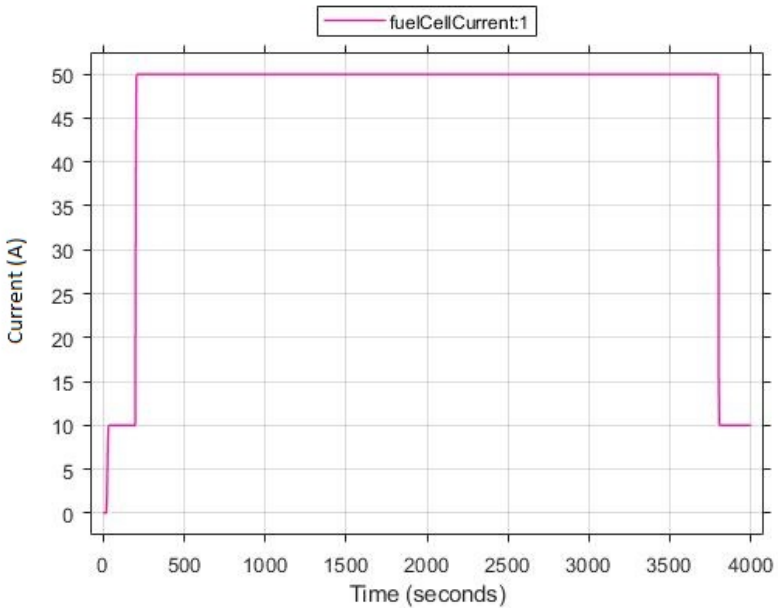

Figure 4.1: The current with unit [A] plotted over time

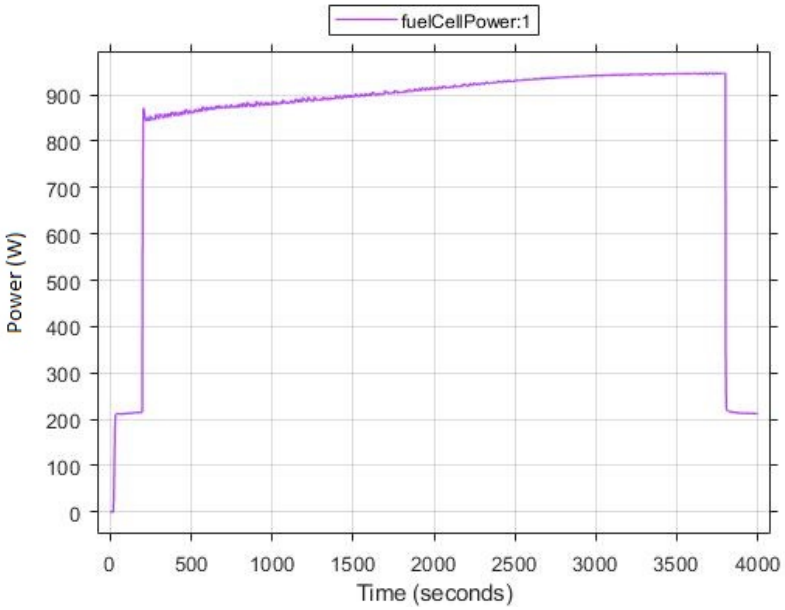

Figure 4.2: The power output in Watt [W] plotted over time

The power rises from around 850W to 950W during the run. This power output results in the figures 4.3 and 4.4 which are the temperature of the fuel cell and the temperature in the chamber respectively.

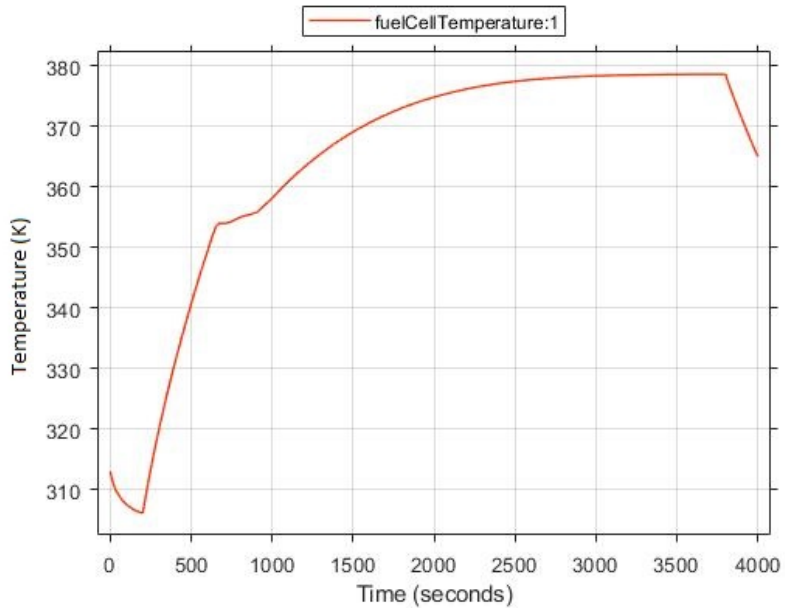

Figure 4.3: Fuel cell Temperature In Kelvin [K] plotted over time

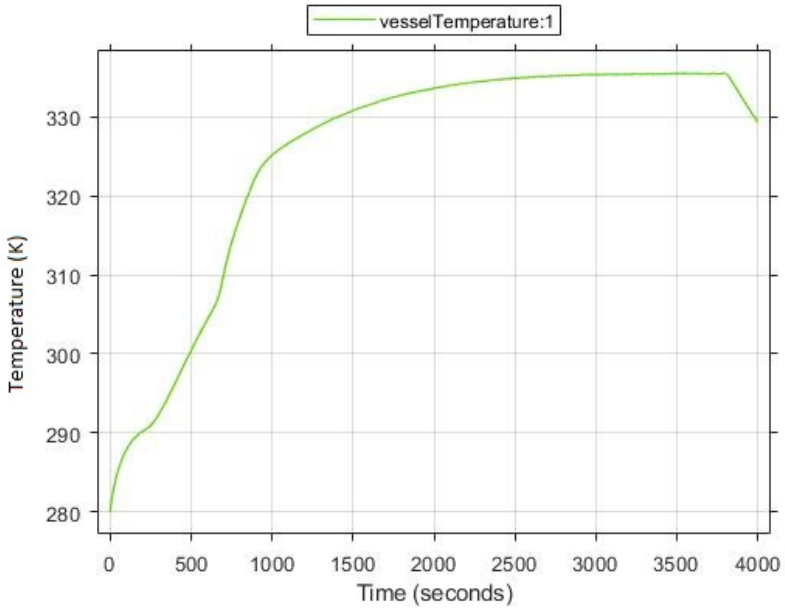

Figure 4.4: Temperature [K] in the chamber plotted over time

The fuel cell temperature is over 100°C and the temperature in the chamber reaches roughly 60°C.

The pressure in the chamber is shown in figure 4.5.

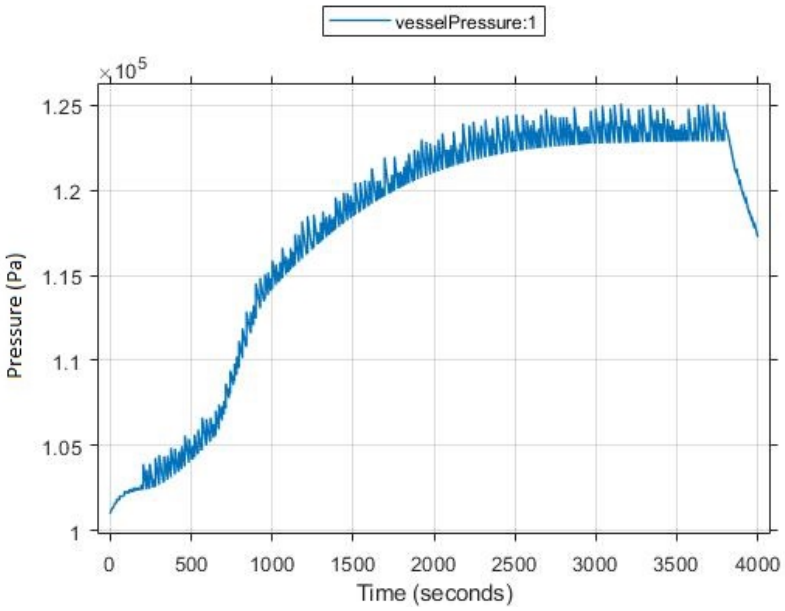

Figure 4.5: Pressure [Pa] in the chamber plotted over time

The pressure inside the chamber reaches roughly 1.25 Bar.

The amount of water inside the chamber can be seen in figure 4.6

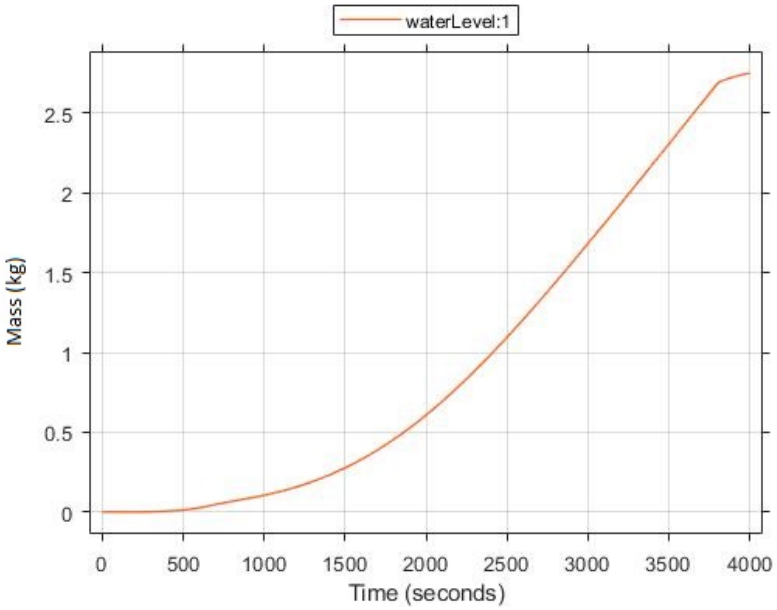

Figure 4.6: Amount of liquid water [kg] in the chamber plotted over time

With the assumption that the density of water is 1000 kg/m^3, the amount of water produced och collected during this run is close to 2.8 dm^3 or 2.8 litres. This equals an increase of water of around 0.7 ml per second.

Run With Low Power Output

During simulation with the current set to 10A the following results is obtained

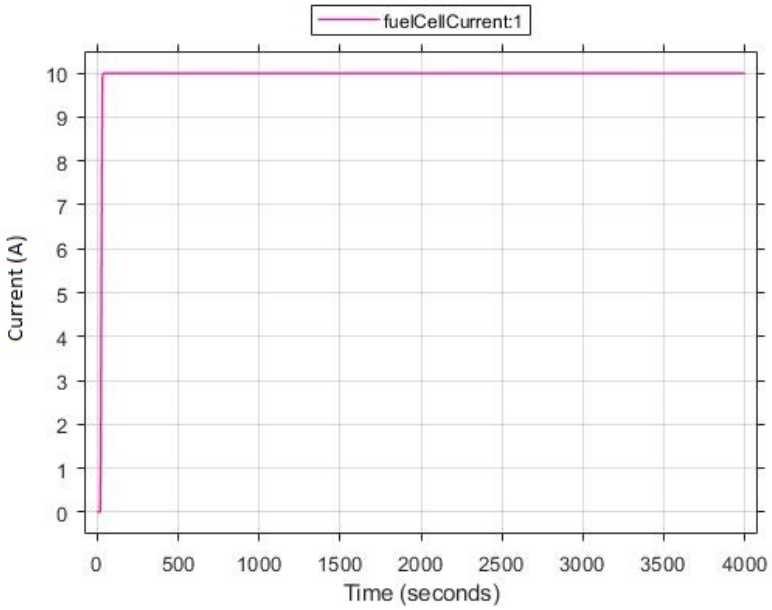

Figure 4.7: The current with unit [A] plotted over time

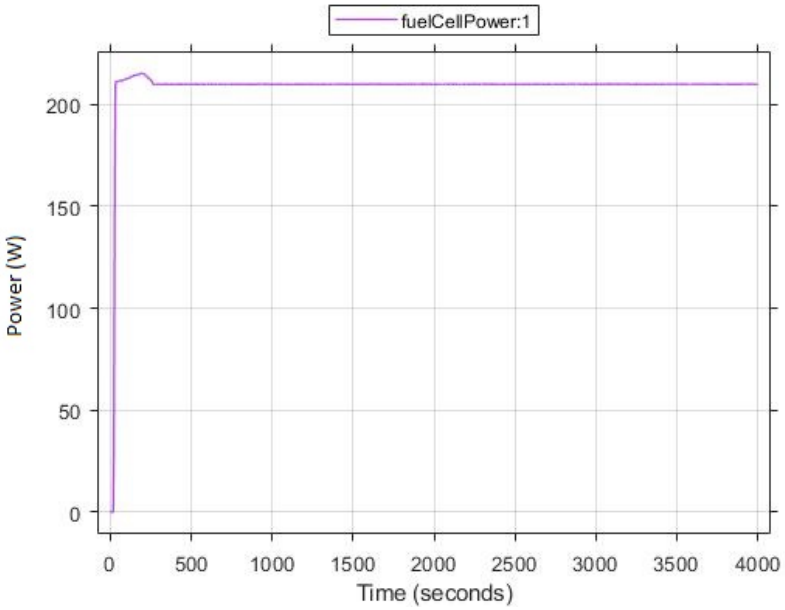

Figure 4.8: The power output in Watt [W] plotted over time

The power overshoots slightly but quickly gets steady around 210 W.

The temperatures of the fuel cell and in the chamber as a result of this power output is shown in figures 4.9 and 4.10 respectively.

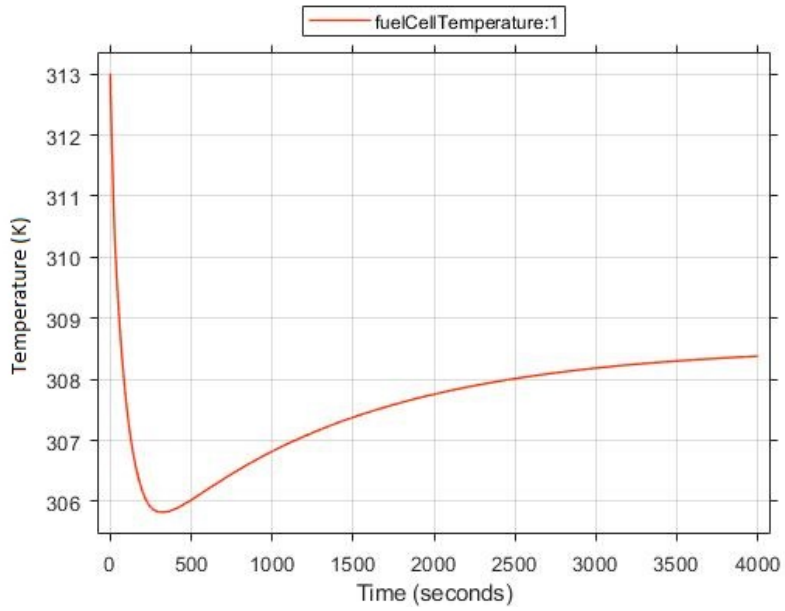

Figure 4.9: Fuel cell Temperature In Kelvin [K] plotted over time

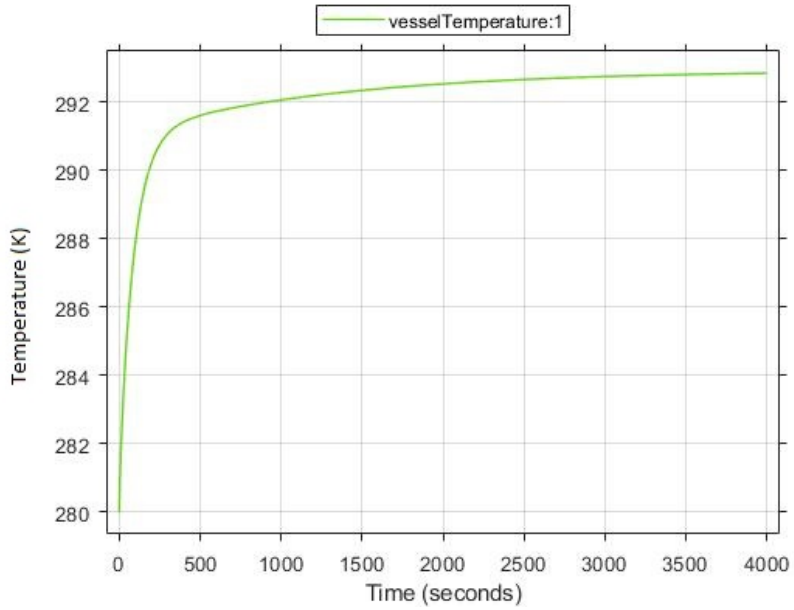

Figure 4.10: Temperature [K] in the chamber plotted over time

The operation temperature of the fuel cell during this low power output does not reach steady state. However, it is close to steady state at around 35°C. The temperature inside the chamber flattens out at approximately 20°C.

The pressure inside the chamber is plotted in figure 4.11.

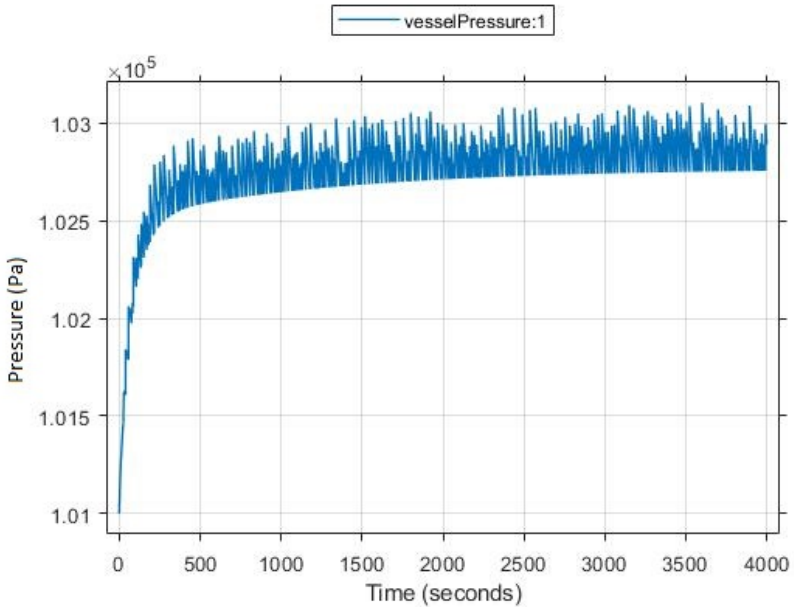

Figure 4.11: Pressure [Pa] in the chamber plotted over time

For low power output, the pressure inside the chamber stays very close to atmospheric pressure during the simulation and tops out at nearly 1.03 Bar.

The collected water during this simulation is shown in figure 4.12.

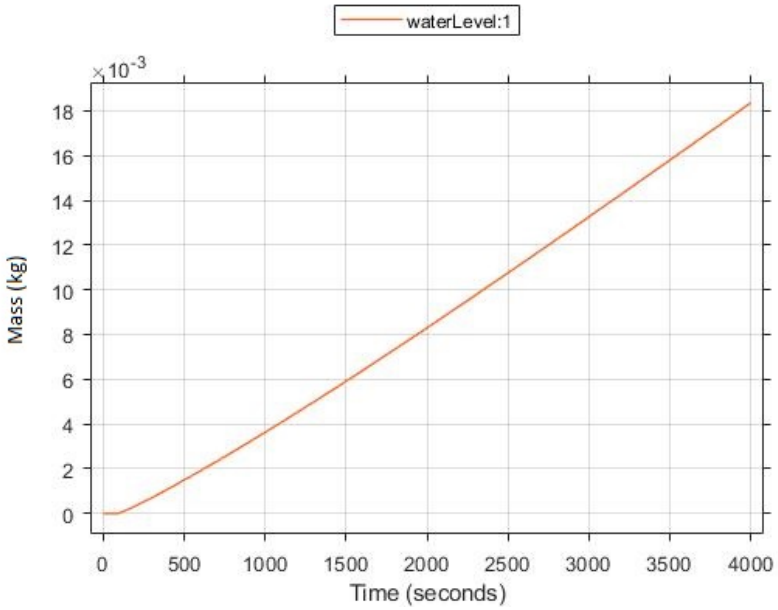

Figure 4.12: Amount of liquid water [kg] in the chamber plotted over time

The amount of water collected in this simulation is close to 0.018 dm^3 and the production of water is roughly 0.0045 ml per second.

Pulsating Run

The current is set to pulsate between 50 and 10 Ampere with a frequency of 1/60 Hertz. The current is plotted in 4.13 and the resulting power output is shown in 4.14.

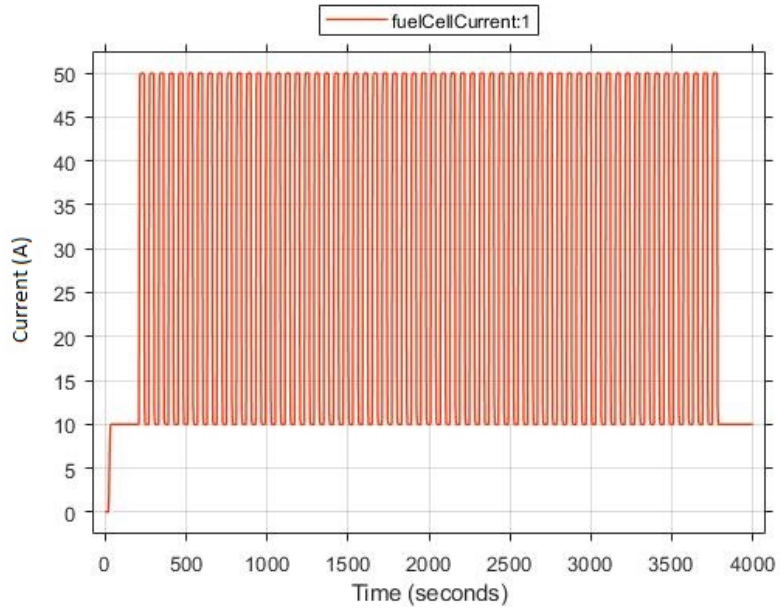

Figure 4.13: Current [A] provided for pulsating run plotted over time

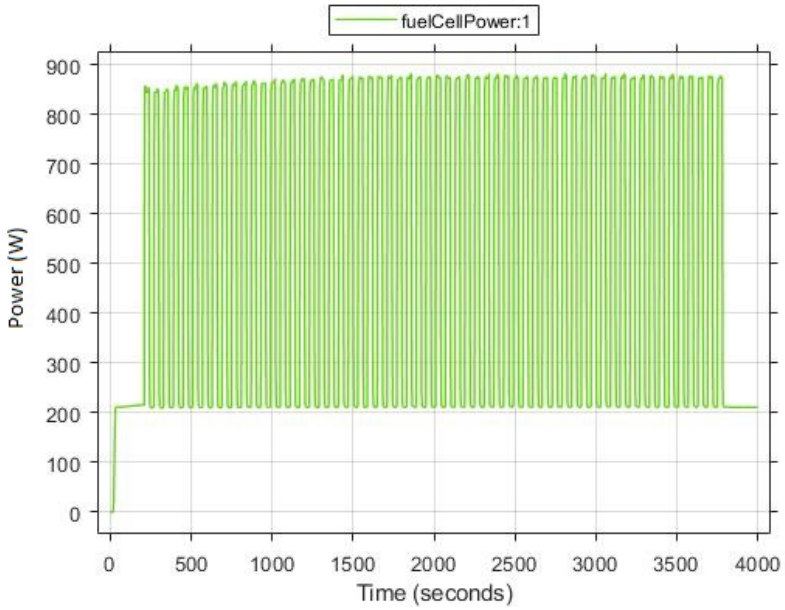

Figure 4.14: The power output in Watt [W] plotted over time

The power output during the high current rises during the simulation but tops out at approximately 880 W. The power output during low current is a bit over 200 W.

The temperature of the fuel cell and the temperature in the chamber is plotted in 4.15 and 4.16 respectively.

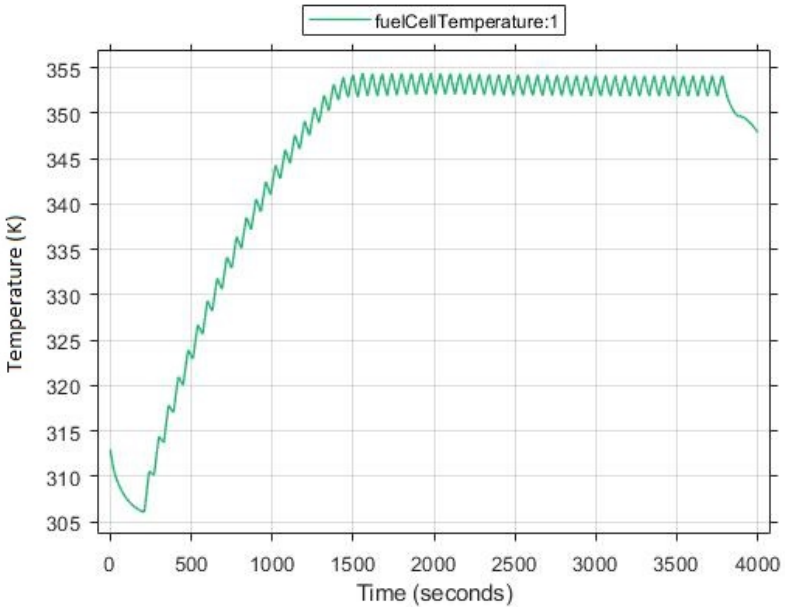

Figure 4.15: Fuel cell Temperature In Kelvin [K] plotted over time

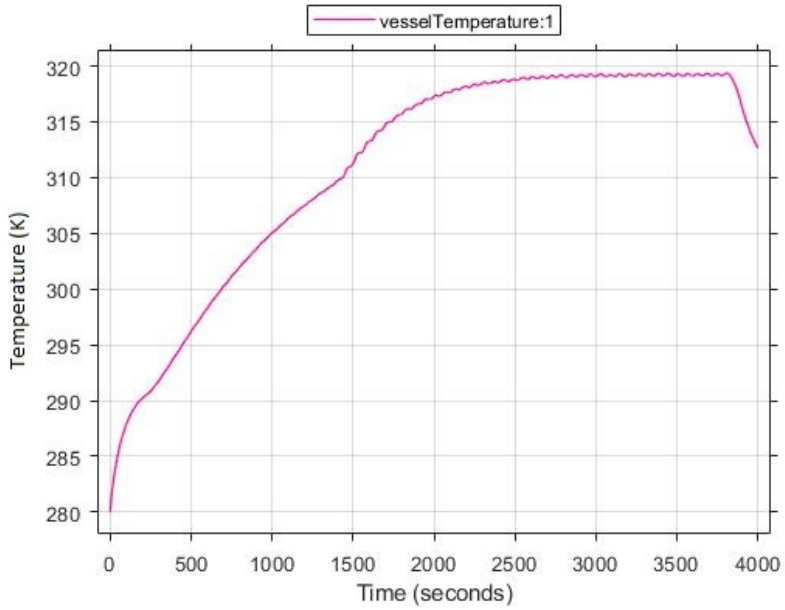

Figure 4.16: Temperature [K] in the chamber plotted over time

The pulsation of the power output is clear in the fuel cell temperature which oscillates during this run. The temperature does however, reach a constant value which it is oscillating around because of the pulse, this value is approximately 80°C. The temperature in the chamber also oscillates but much less than the fuel cell temperature. The chamber temperature reaches a fairly stable temperature of about 46°C.

The pressure inside the chamber is plotted in 4.17.

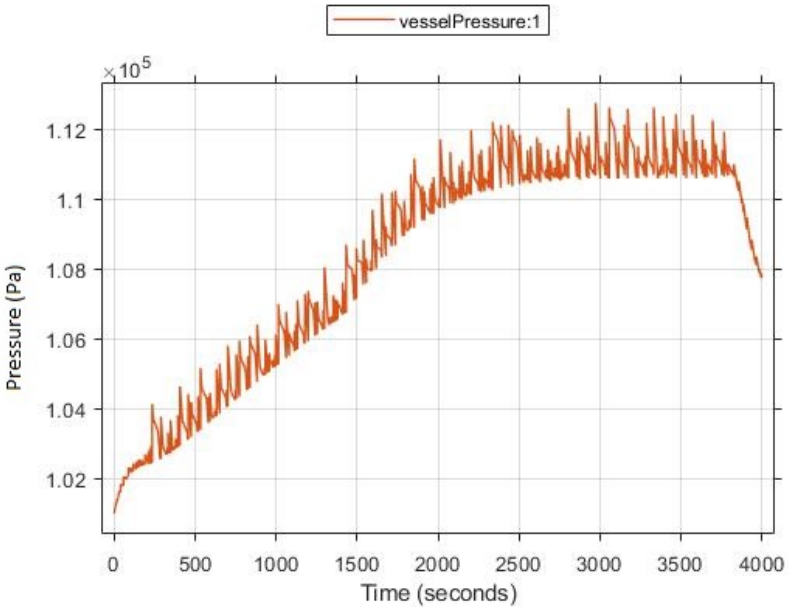

Figure 4.17: Pressure [Pa] in the chamber plotted over time

The chamber pressure follows a similar path as the chamber temperature and tops out at nearly 1.2 Bar.

The amount of water collected in the chamber during this run is plotted in 4.18.

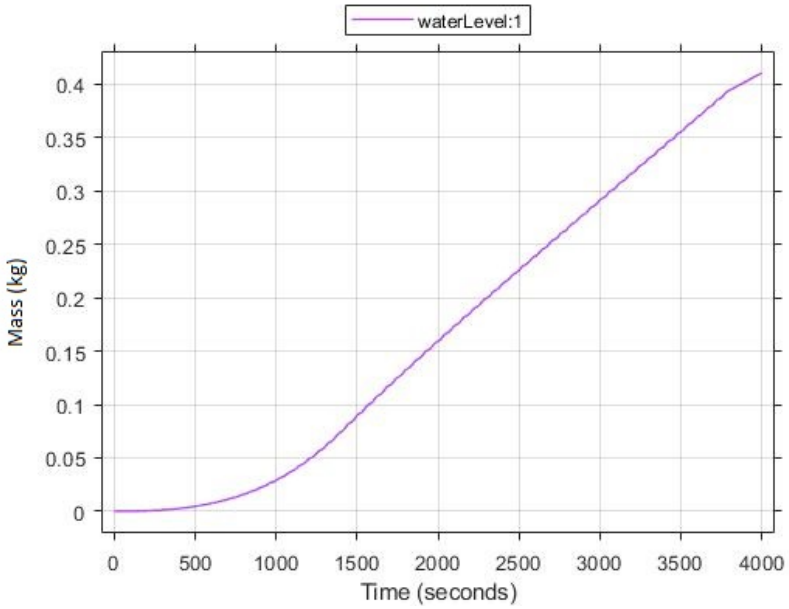

Figure 4.18: Amount of liquid water [kg] in the chamber plotted over time

The amount of water in the chamber just about exceeds 0.4 kg or 0.4 dm^3. This means a production of water of roughly 0.1 ml per second.

Realistic Run

During the realistic run, the current rises for short periods causing a quick burst of power output. The current is shown in 4.19 and results in the power output shown in 4.20.

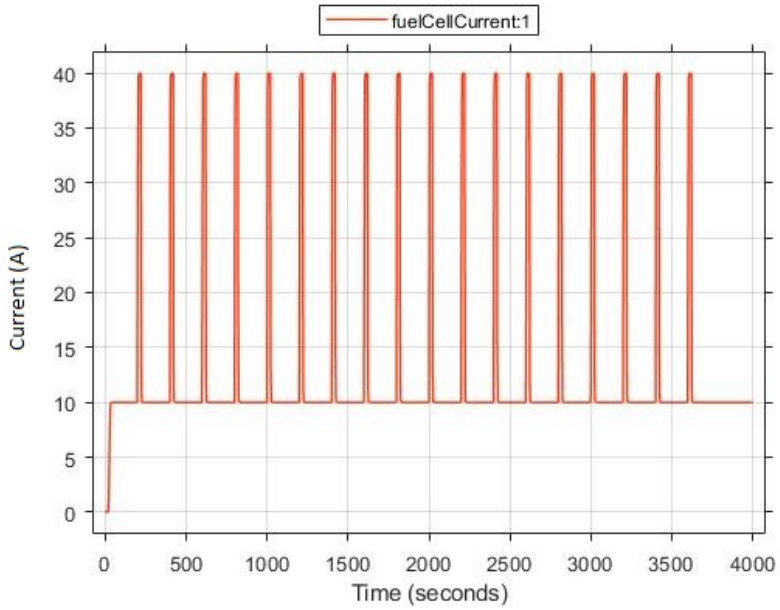

Figure 4.19: The current with unit [A] plotted over time

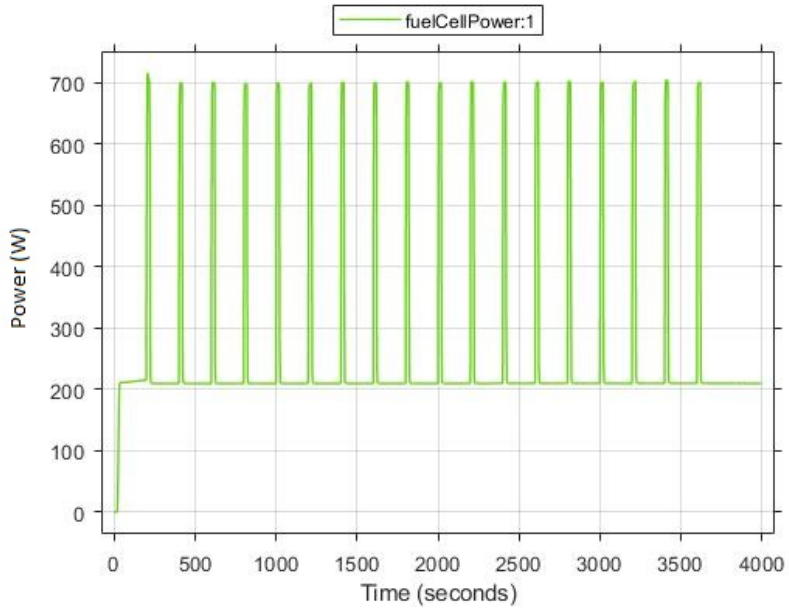

Figure 4.20: The power output in watt [W] plotted over time

The current is set to a constant 10 Ampere that rises to 40 Ampere for 20 seconds every 200 seconds. The resulting power output reaches 700 W during peaks and stays slightly above 200 W during low current.

The fuel cell temperature for this simulation is plotted in 4.21 and the temperature inside the chamber is plotted in 4.22.

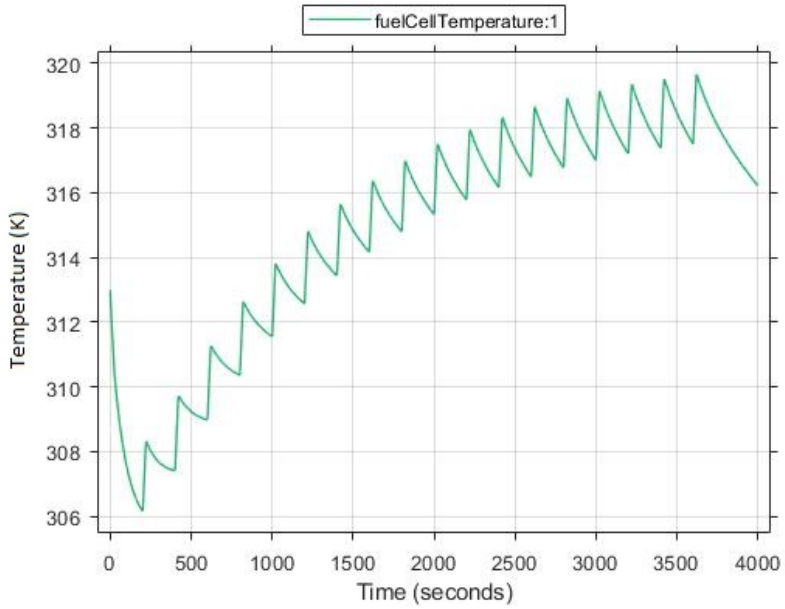

Figure 4.21: Fuel cell Temperature In Kelvin [K] plotted over time

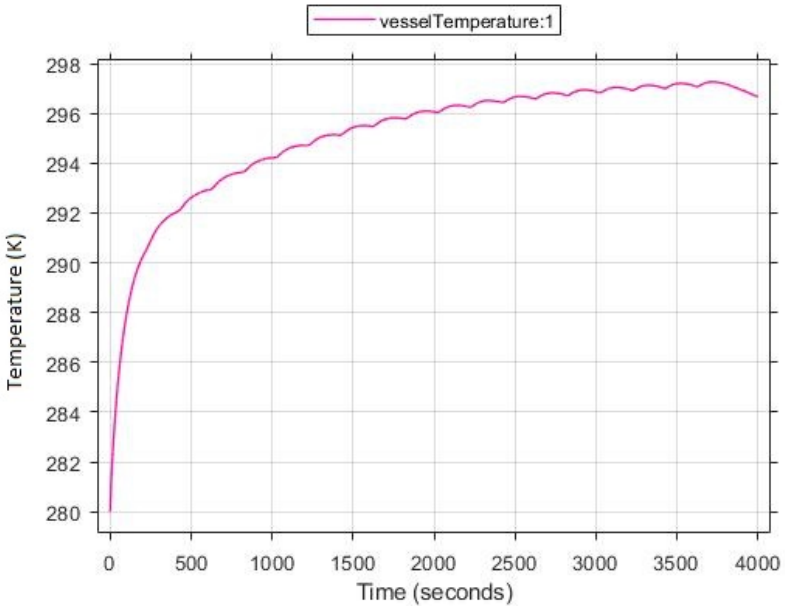

Figure 4.22: Temperature [K] in the chamber plotted over time

Both the temperature of the fuel cell and in the chamber oscillates but the fuel cell temperature has a bigger amplitude. The fuel cell temperature reaches 45°C but might increase slightly more for a longer simulation. The temperature inside the chamber might also ini-

crease slightly for a longer run but during this simulation it tops out at nearly 25°C.

The pressure inside the chamber is plotted in 4.23.

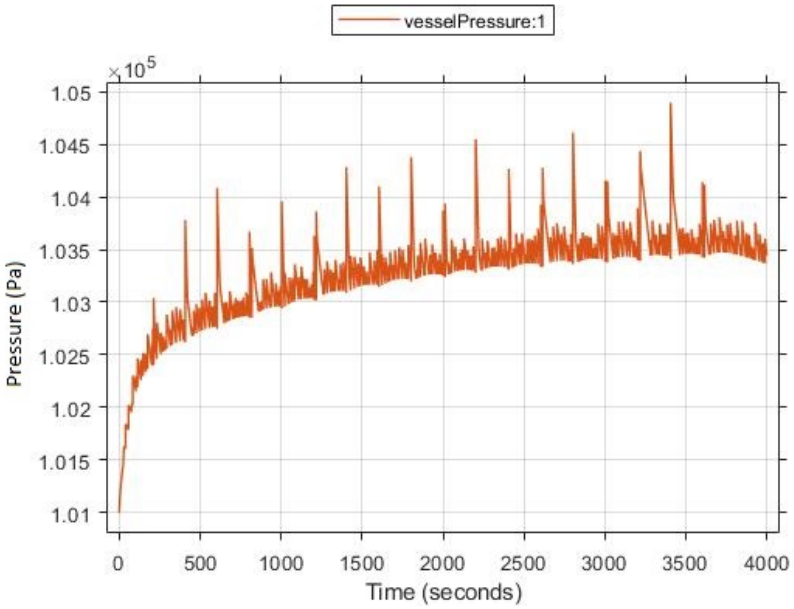

Figure 4.23: Pressure [Pa] in the chamber plotted over time

The peaks of power output is clearly visible in the resulting pressure in the chamber. During one of the peaks, the pressure almost reaches 1.05 Bar which is still close to atmospheric pressure.

The amount of water collected in the chamber during this run is plotted in 4.24.

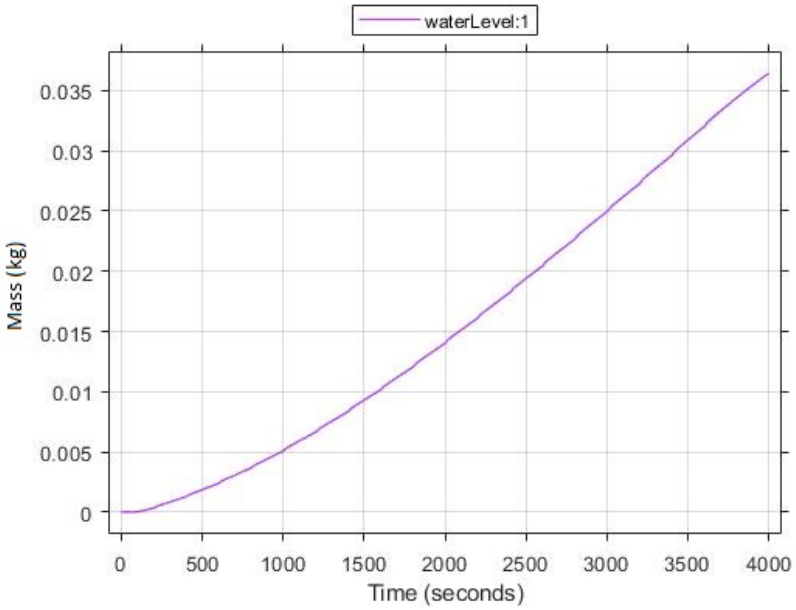

Figure 4.24: Amount of liquid water [kg] in the chamber plotted over time

The collected water amounts to approximately 0.036 kg water which is 0.036 dm^3. This equals an increase of water at around 0.009 ml per second.

No Power Output

In this scenario, the current is set to give a low power output for 90 seconds and than go to no power output for a long period of time. The power output is plotted in 4.25.

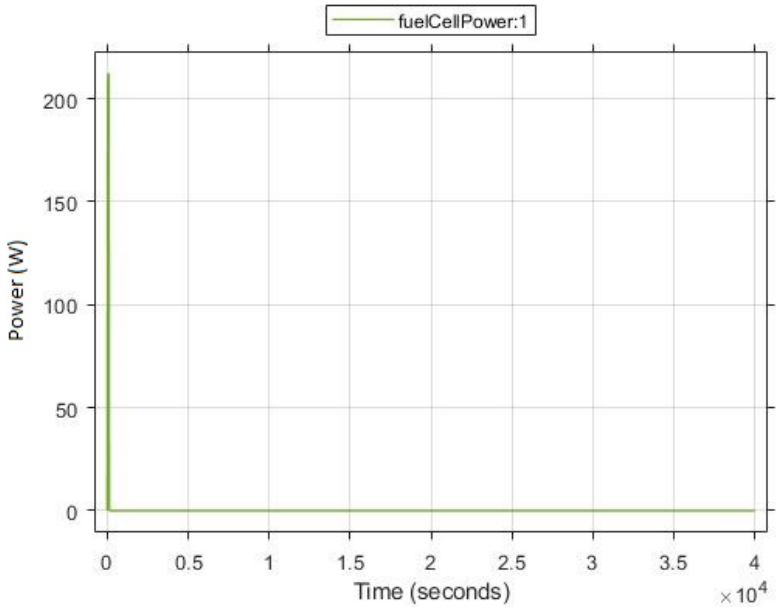

Figure 4.25: The power output in watt [W] plotted over time

When there is no power output the results of the different temperatures, the pressure and amount of water inside the chamber is shown in the graphs below.

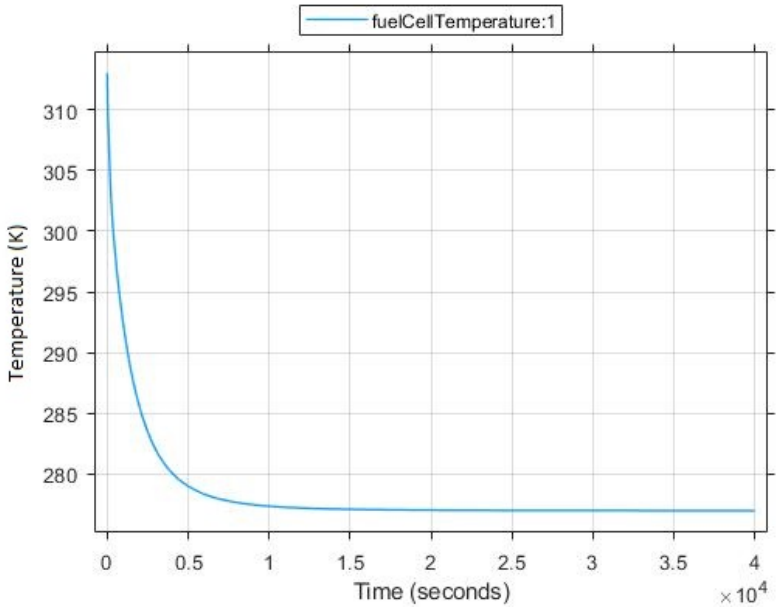

Figure 4.26: Fuel cell Temperature In Kelvin [K] plotted over time

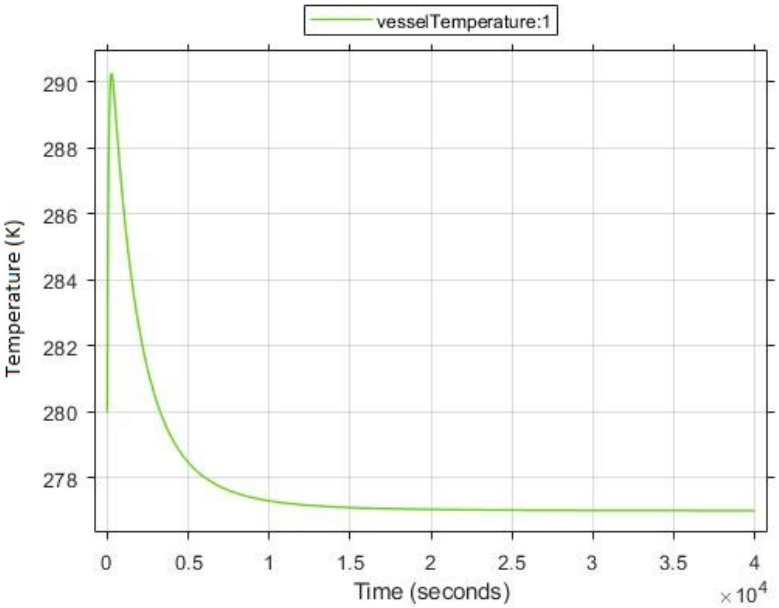

Figure 4.27: Temperature [K] in the chamber plotted over time

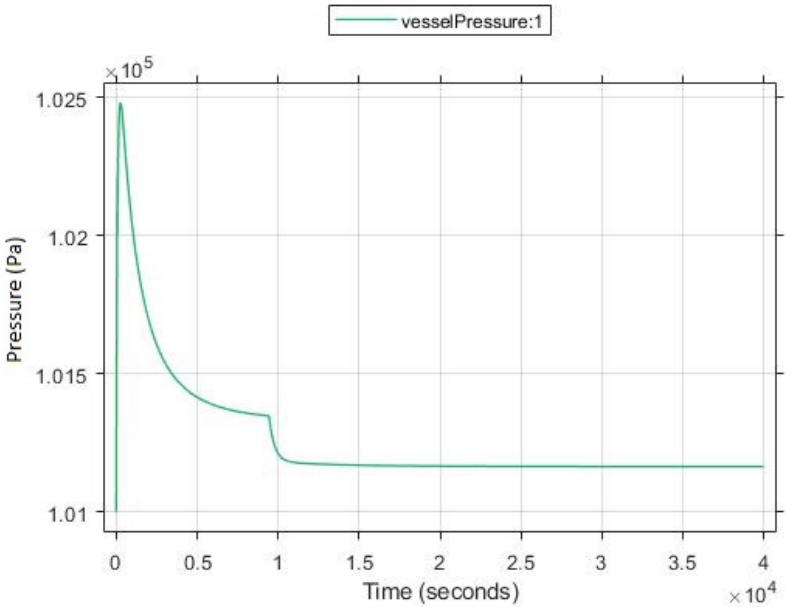

Figure 4.28: Pressure [Pa] in the chamber plotted over time

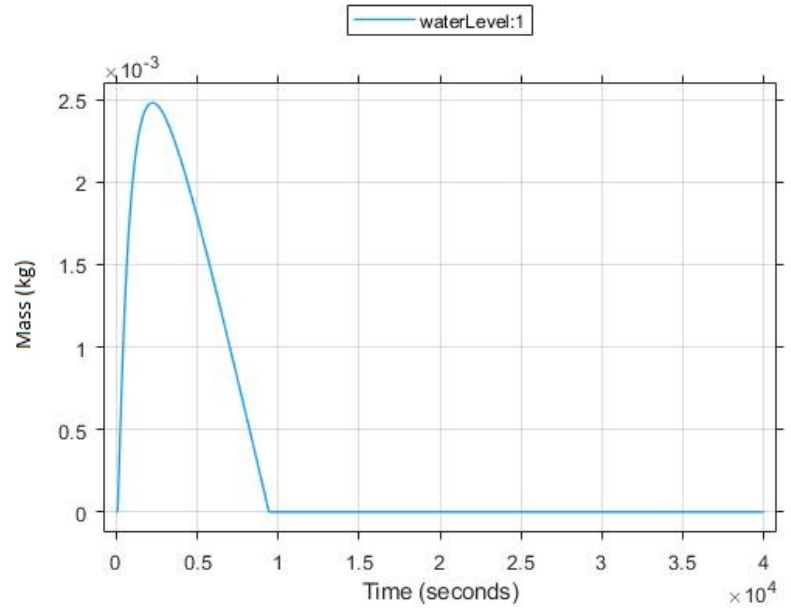

Figure 4.29: Amount of liquid water [kg] in the chamber plotted over time

Start and Shut-Down

The result from the implementation of start and shut down procedure is shown in this section.
In figure 4.30, the applied current is shown. The current is arbitrarily set and is set to start after a few seconds in order to allow the hydrogen to replace the air in the anode.

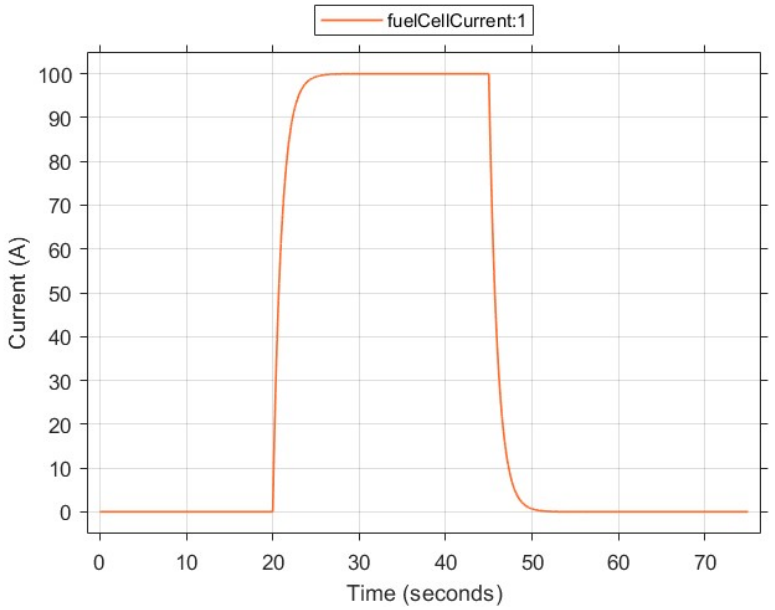

Figure 4.30: The current with unit [A] plotted over time

During the first part of the simulation, a flow of hydrogen is added to the anode and the air is depleted from the anode. For the last part of the simulation, the hydrogen is depleted and air is introduced to the anode. This leads to figures 4.31 and 4.32.

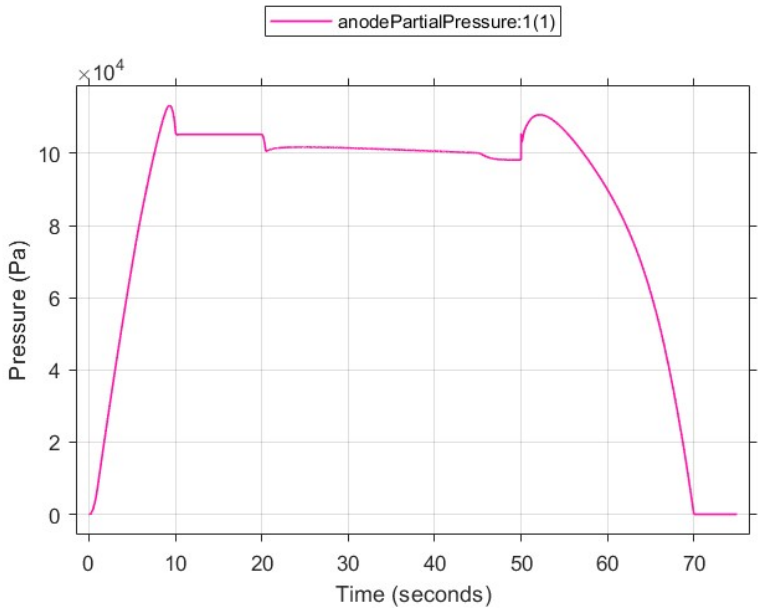

Figure 4.31: The hydrogen partial pressure [Pa] in the anode plotted over time

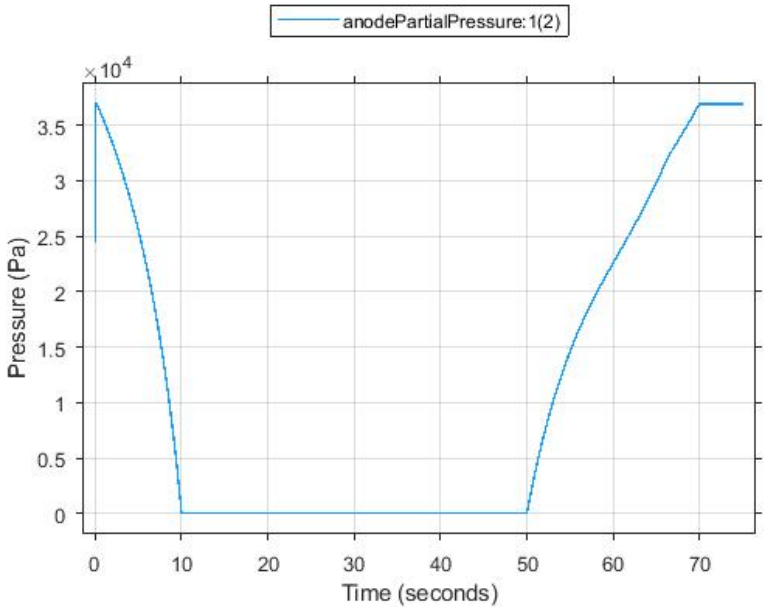

Figure 4.32: The oxygen partial pressure [Pa] in the anode plotted over time

The resulting voltage in a single cell is shown in figure 4.33.

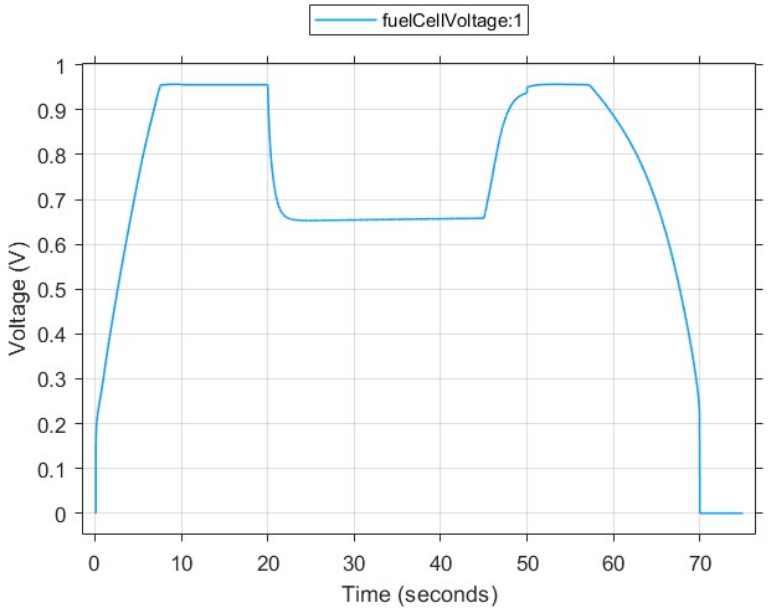

Figure 4.33: The voltage produced by a single cell [V] plotted over time

4.2 Control

Anode and Cathode Pressure

The resulting difference in the anode and cathode pressure is shown in this section.

In figure 4.34 the pressure difference is shown during a pulsating current of between 50 and 30 Ampere.

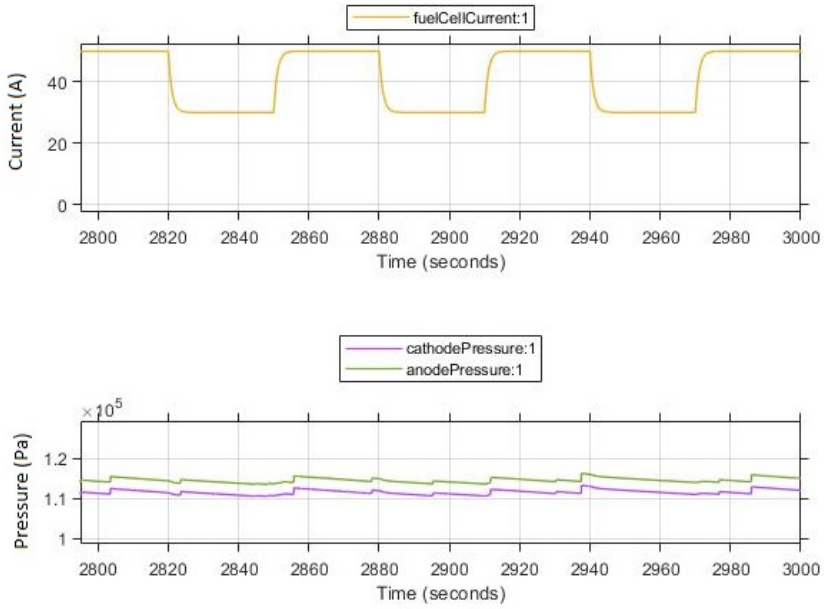

Figure 4.34: Resulting pressure difference [Pa] from set current [A]

The pressure difference stays constant and in 4.35 the pressure difference during a step increase and decrease of the current is shown.

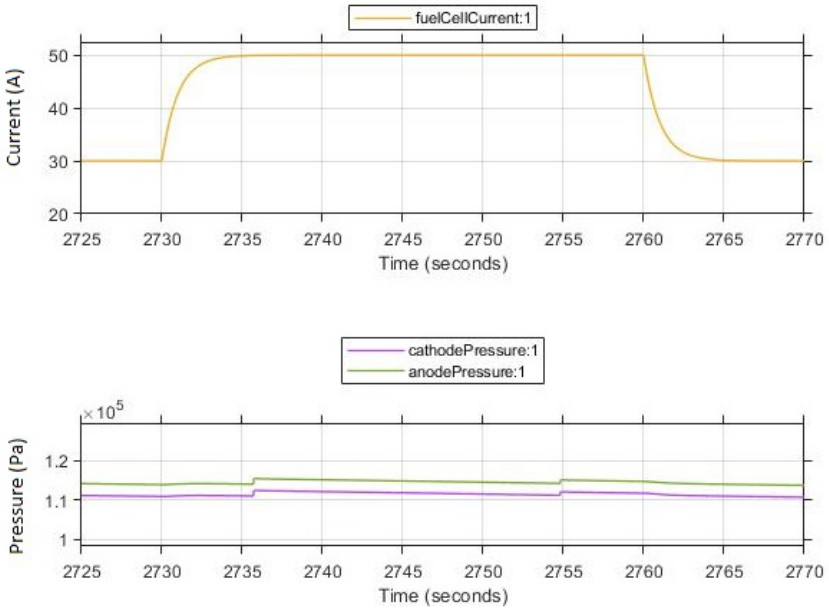

Figure 4.35: Pressure difference during a step

The pressure differences for the case with high power output and the realistic power output case is shown in 4.36 and 4.37 respectively.

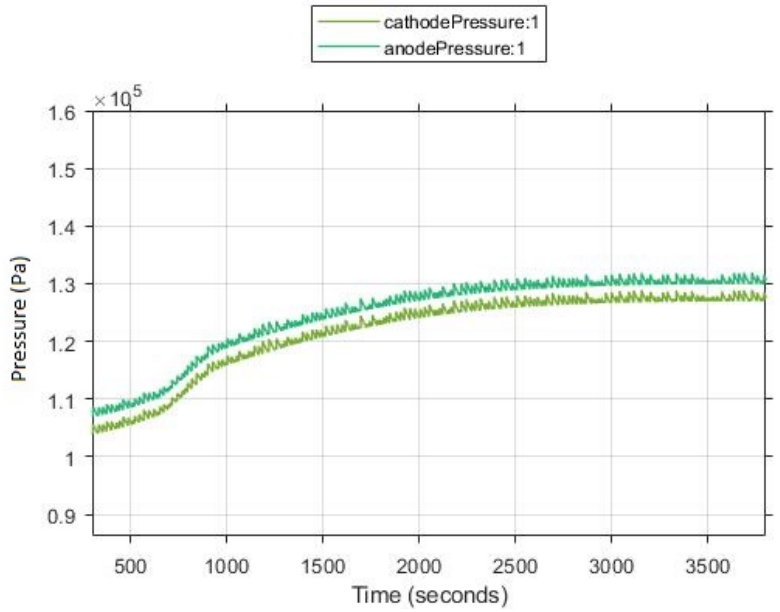

Figure 4.36: Pressure difference during the high power output scenario

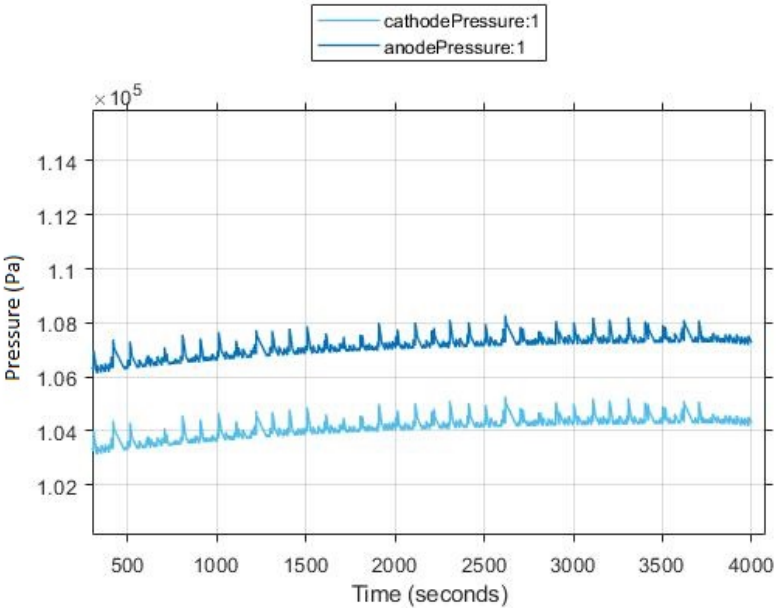

Figure 4.37: Pressure difference during the realistic power output scenario

During both of these runs, the pressure difference stays constant at the desired difference.

Oxygen Partial Pressure

The valve from the oxygen tank was controlled by the partial pressure of oxygen inside the chamber. In the figures below the result of this pressure is plotted for the different scenarios.

The partial pressure of oxygen inside the chamber for the low power output scenario is shown in figure 4.38.

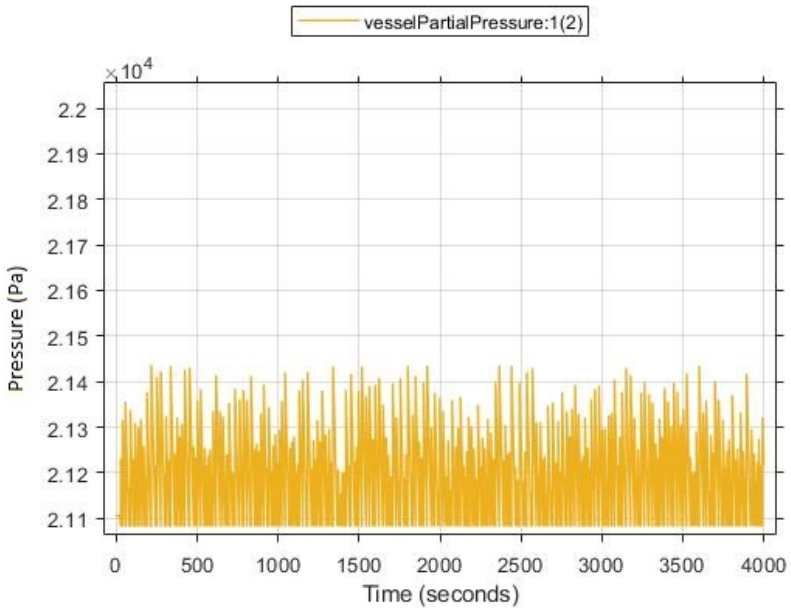

Figure 4.38: Partial pressure [Pa] of oxygen in the chamber during low power output plotted over time

The partial pressure of oxygen is noisy but it does stay close to the reference pressure with a maximal difference of around 0.4 kPa.

The partial pressure of the oxygen during the scenario with high power output is shown in figure 4.39.

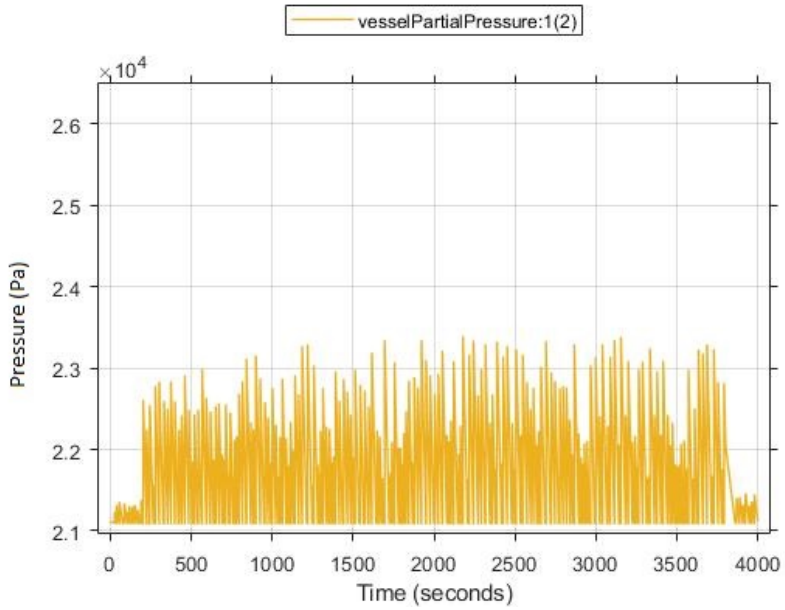

Figure 4.39: Partial pressure [Pa] of oxygen in the chamber during high power output plotted over time

The partial pressure of oxygen deviates with around 2.5 kPa from the reference pressure.

For the scenario with pulsating power output, the resulting partial pressure of oxygen inside the chamber is plotted in 4.40.

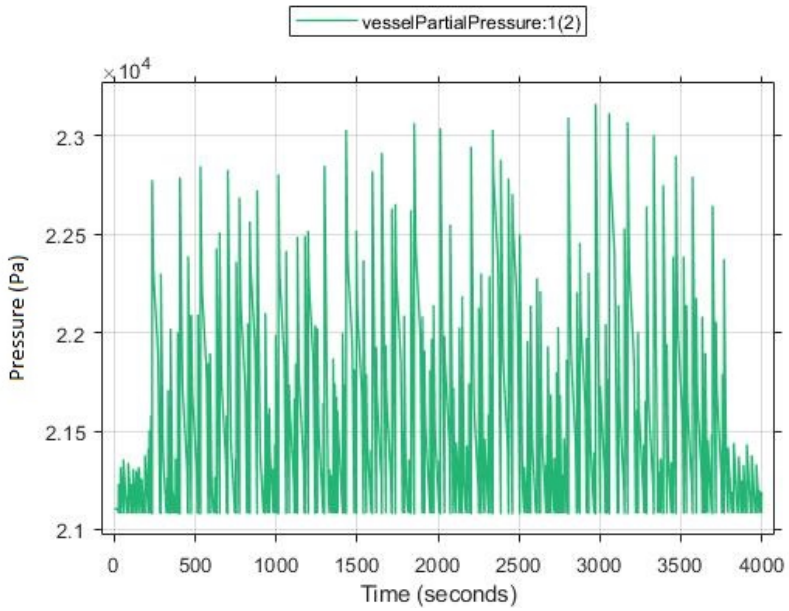

Figure 4.40: Partial pressure [Pa] of oxygen in the chamber during the pulsating scenario plotted over time

During this scenario, the pressure deviates with approximately 2 kPa from the desired pressure.

Lastly, the oxygen partial pressure during the realistic scenario is plotted in 4.23.

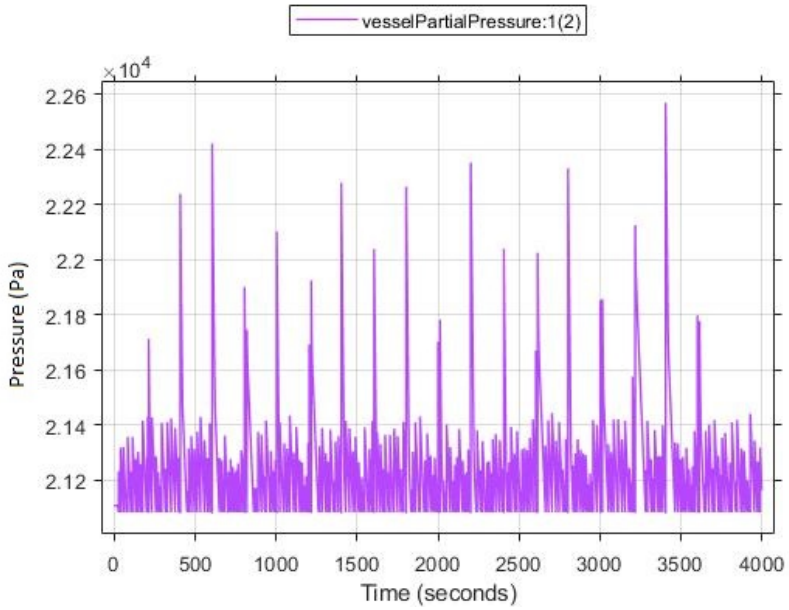

Figure 4.41: Partial pressure [Pa] of oxygen in the chamber plotted over time

The pressure difference between the maximal pressure and the desired pressure is roughly 1 kPa during this scenario.

5 Discussion

This chapter contains discussion about the results.

5.1 Modelling

The results of the simulation model seems to be realistic and intuitive which is positive. However, there have been no validation and it would be preferred to test the real system in order to validate the simulation data with measured data. Ideally, the fuel cell, the compressor and the hydrogen blower should be tested separately and together in the full system.

The modelling of the thermal management gives intuitive temperature data during simulations. Depending on the intended power output during real runs an air cooling solution could be considered. However, since the fuel cell temperature reaches high temperatures during longer high power output simulations, the coolant loop solution is most likely the best way to cool the fuel cell.

5.2 Results

In this section the results from the simulations and the simple control strategy will be analyzed and discussed.

Simulations

In general, the results from the different scenarios seem to follow the expectations in that, for example, the fuel cell temperature increases for increasing power output.
Taking a closer look at the scenario with high power output shows that the fuel cell temperature grows until around 105°C. Considering that the usual operating temperature of a LT-PEMFC is around 60-80°C and a temperature higher than 100°C will cause the membrane to dry up [5], a high power output should be limited to short time periods. At approximately 750 seconds there is a small plateau at roughly 353 Kelvin before it rises again. This is the reference fuel cell temperature and the system tries to maintain this temperature but the cooling can not handle the workload and the temperature rises past it. The power output increases for the duration of the simulation, the reason for this is that the losses decreases with increasing fuel cell temperature and increasing anode and cathode pressure. The temperature inside the chamber during the high power output scenario reaches approximately 62°C which is close to the advised maximum ambient temperature of around 70°C.
For the scenario with low power output, the fuel cell temperature only reaches 35°C, which is lower than the typical operating temperature. Comparing the temperature inside the

chamber for the low power output scenario with the high power output scenario the temperature is roughly 40°C lower and only gets to 20°C. There is no problem with the chamber temperature, however, the fuel cell temperature is well below the usual working temperature.

The pressure inside the chamber for the high power output is close to 1.25 Bar at the end of the run. This is an increase of around 0.24 Bar to atmospheric pressure which is fairly big. The oscillations mainly comes from the partial pressure of oxygen. This should not, however, be an issue for the real application since the fuel cell can operate with an ambient pressure of up to 1.5 Bar. For the pressure inside the chamber during low output the pressure barely increases from the atmospheric pressure and should not cause any problems.

The increase of water is 155 times larger per second in the high output, which is 0.7 ml per second, compared to the low output. With an increase of 0.7 ml per second it would take almost 43 hours at maximum capacity to fill the chamber of 108 litres to the top.
The increase in water is not linear which is because the pressure and temperature inside the chamber controls the water production. For constant pressure and temperature, the increase of water would be linear.

The pulsating run is mainly interesting to analyze for the control of the hydrogen and oxygen flow, which will be discussed in section 5.2. But it is also interesting to compare it to constant current to investigate any differences. It is clear that the pulse of current affects the fuel cell temperature which now oscillates while it did not for the constant currents. As a result of the oscillation in the fuel cell temperature, the chamber temperature also oscillates. This is intuitive since the oscillation of fuel cell temperature would cause the temperature of the coolant liquid to oscillate which in turn would cause the oscillation of the temperature inside the chamber. The oscillation in chamber temperature does not have as much amplitude as for the fuel cell because the time it takes to heat and cool the air inside the chamber is longer than for the fuel cell. It was also clear that the water increase was larger for higher power output which should cause some oscillation in the water amount as well. The pulse causes a slope that would be the result of a constant current with the value of somewhere between 50 and 10 Ampere.

For the realistic run, the results is in line with the other results and follows intuition. The fuel cell temperature is 45°C which is higher than for the low power output but lower than for the high and pulsating power output. 45°C is lower than the advised working temperature which is not optimal but it should not cause problems. The temperature and pressure inside the chamber stays close to atmospheric conditions and should also not be a problem. Whether or not this power output is actually realistic will be discussed in section 5.3.

From the no power output scenario some results is examined. The temperature in the chamber and the fuel cell temperature both goes towards 277 Kelvin, this is the assumed temperature outside of the chamber which means the temperature in the submarine eventually reaches the same temperature as the surrounding temperature. The sudden drop in pressure inside the chamber at approximately 1000 seconds is caused by the complete depletion of liquid water.
Mainly, the results from this scenario is of interest in the discussion about whether to shut the fuel cell down or to produce very low power. If there is not any need for power from the fuel cell, the obvious solution is to shut down the fuel cell. A further investigation on the impact of shut down and start up together with the impact off low power output on the fuel cell is of interest in order to maximize the lifespan of the fuel cell. Another negative with shutting down and starting up the fuel cell is the fact that the submarine will be far from anyone that can physically interact with it if anything goes wrong. The procedures for starting and

shutting down the fuel cell is a little intricate and should anything go wrong it could lead to a malfunctioning fuel cell or in worst case a lost submarine.

From the results for the start and stop simulations there are some observations of interest. Broadly, it can be said the results matches the expected results.
The hydrogen partial pressure starts to increase directly when hydrogen is introduced to the anode in replacement of air, while the oxygen partial pressure decreases. After approximately 8 seconds the fuel cell is in the Open Circuit Voltage (OCV) state before a current of 100 A is applied after 20 seconds in a step which results in a power output and the system leaves the OCV state. At 45 seconds the current is lowered to zero in a step and aa it enters the OCV state at 50 seconds, the hydrogen starts to deplete from the anode while air is introduced.
The cell voltage increases at the start when air is replaced with hydrogen. At 20 seconds the voltage decreases following the connected current load, which is constant until 45 seconds. At 45 seconds the current is disconnected leading to an increase in cell voltage. At 50 seconds the hydrogen starts to be replaced with air which lowers the cell voltage. At both the start and the end there is a very steep change when the hydrogen pressure is close to zero, meaning that the model is very sensitive for small hydrogen pressures.

Control

The hydrogen supply valve was controlled to maintain constant pressure difference between the anode and the cathode. During all simulations the pressures keeps at a constant desirable difference. For pulsating current the pressures follows each other fast as can be seen in the results from the pulsating scenario but also the realistic scenario where the current suddenly increase. The PID-regulator can control the valve for the hydrogen flow and output desired values.

The valve that controls the oxygen supply to the chamber is controlled to maintain a constant oxygen partial pressure inside the chamber. This pressure is fairly close to desirable during all simulations, the biggest difference between the desired value and simulated value is only 2.5 kPa during the high power output scenario.

5.3 Method

One problem with the method in this thesis is the lack of validation. The results from the simulations can be compared to the data sheets provided by the production companies but an experimental investigation would be necessary to validate the models. All parts of the system should preferably be validated alone and in the full system. For example, the compressor should be validated by comparing measured data from an experiment with simulation data for the same inputs. It would also be favourable to test the full fuel cell system in a chamber and tune the inputs in the simulation to emulate the experimental conditions and compare the collected data.

The scenarios used for the simulations are mainly extreme cases and provide interesting information. However, the scenario labeled as 'realistic' is close to a guess and follows many assumptions. An actual realistic scenario might be vastly different from this and therefore a more fair name for that scenario would be small bursts of high power output. The results obtained from this scenario is still of interest and provides knowledge of how the system behaves but the claim that it is a realistic scenario could be questioned.

6 Future Work

To validate the model brought forward in this project, an experimental measurement of the real system is necessary. The model can be adjusted to emulate the conditions during the experimental tests. The model includes a few assumptions on the different lengths of tubes meaning that some volumes may differ from those in the real system. For the hydrogen blower and the compressor, even though the model follows the data acquired from the companies producing them, a test to verify the data sheets is preferable.

Since there are not any standards in velocity profiles for submarines, the power output scenarios have only been used to understand how the system will react during different requirements. It would be beneficial to investigate what the velocity of the submarine is supposed to be during a simple run, calculate the required power output for that and control the provided current to generate the desired power output.

The control of the valves that regulates the hydrogen and oxygen flow is very simple. For the purposes of this project, the results of it is acceptable and not much time has been spent trying to improve it. It is possible that a more sophisticated solutions will yield better results and should therefore be investigated more thoroughly.

An investigation on how starting up and shutting down a fuel cell affects the degrading of the fuel cell and how many of these start and stops it can tolerate would be beneficial. It would also be of interest to investigate if starting and shutting down the fuel cell remotely is possible or if the risk involved is too high. It would also be of interest to investigate how constant low power output affects the fuel cell since the working temperature is lower than advised during these simulations.

7 Conclusion

In this thesis a submarine powered by a fuel cell has been modeled with the purpose to use it for simulations in order to analyze how the conditions will be during real runs. To regulate the external hydrogen and oxygen flow, a simple control strategy has been used.

The developed model of the fuel cell system gives reasonable values during simulations and changing, for example, the provided current to a lower value lowers the power output from the fuel cell. Changes made in parameters intuitively converts the resulting outputs. However, the lack of validation for the model makes it unreliable and further investigation is necessary.
So to answer the first research question "Can the system be modeled to accurately represent the application?". No, the model in this project can not be said to accurately represent the application due to the lack of validation.

With a simple PID-regulator, the system works and in this thesis it was shown that the oxygen partial difference and the pressure difference between the anode and cathode follow desired values. An investigation on an more optimal way to control the hydrogen and oxygen flow would be beneficial but to answer the second research question, "Can PID-regulators be used to control hydrogen and oxygen flow?". Yes, PID-regulators can be used to control these flows and the results are satisfactory.

This thesis has included an investigation on whether there will be any thermal implications for the submarine during runs. For long, high power output runs, the fuel cell temperature exceeds advised temperatures and the temperature inside the fuel cell nearly reaches critical temperature. It is, however, unlikely that the fuel cell would need to provide that power output for long periods of time, helped by the fact that the submarine will be an electric/fuel cell hybrid.
This answers the last research question, "What is the thermal limitations of the system?". The system is limited by thermal limitations during long, high power output runs. For realistic power outputs however, it should not limit the system.

Bibliography

[1] R. d'Amore-Domenech & M.A. Raso & A. Villalba-Herreros & O. Santiago & E. Navarro & T.J Leo. "Autonomous underwater vehicles powered by fuel cells: Design guidelines". In: *Ocean Engineering* 153 (2018), pp. 387–398. DOI: https://doi.org/10.1016/j.joceaneng.2018.01.117.

[2] Whitney G. Colella & Fritz B. Prinz & Ryan O'Hayre & Suk-Won Cha. *Fuel Cell Fundamentals*. John Wiley & Sons, inc, 2016. ISBN: 9781119113805.

[3] Engineers Edge. *Horizontal Cylinder Natural Convection Equation and Calculator*. URL: https://www.engineersedge.com/heat_transfer/horizontal_cylinder_natural_convection_13970.htm. (accessed: 15.09.2023).

[4] Berna Sezgin & Y. Devrim & T. Ozturk & I. Eroglu. "Hydrogen energy systems for underwater applications". In: *Inernational Journal of Hydrogen Energy* 47 (2022), pp. 19780–19796. DOI: https://doi.org/10.1016/j.ijhydene.2022.01.192.

[5] R. Rosli & A. Sulong & W. Daud & M. Zulkifley & T. Husaini & M. Rosli & E. Majlan & M. Haque. "A review of high-temperature proton exchange membrane fuel cell (HT-PEMFC) system". In: *International Journal of Hydrogen Energy* 42.14 (2017), pp. 9293–9314. DOI: 10.1016/j.ijhydene.2016.06.211.

[6] Helge Weydahl & M. Gilljam & T. Lian & T.C. Johannessen & S.I. Holm & J.O. Hasvold. "Fuel cell systems for long-endurance autonomous underwater vehicles - challenges and benefits". In: *Internation Journal of Hydrogen Energy* 45 (2020), pp. 5543–5553. DOI: https://dx.doi.org/10.1016/j.ijhydene.2019.05.035.

[7] Oistein Hasvold and N.J. Storkersen. "Electrochemical power sources for unmanned underwater vehicles used in deep sea survey operations". In: *Journal of Power Sources* 96 (2001), pp. 252–258. DOI: https://doi.org/10.1016/S0378-7753(00)00685-6.

[8] Alejandro Mendez & Teresa Leo & Miguel Herreros. "Current State of technology of Fuel Cell Power Systems for Autonomous Underwater Vehicles". In: *Energies* 7 (2014), pp. 4676–4693. DOI: https://doi.org/10.3390/en7074676.

[9] J.P. Holman. *Heat Transfer*. ISBN: 0-07-029620-0.

[10] https://commons.wikimedia.org/wiki/User:Turbojet. *Alkaline fuel cell*. URL: https://commons.wikimedia.org/wiki/File:Alkaline_fuel_cell_%28ro%29.png.

[11] James Larminie and Andrew Dicks. *Fuel Cell Systems Explained*. J. Wiley, 2003. ISBN: 978-0-470-84857-9.

[12] Xiaoming Wang & J. Shang & Z. Luo & L. Tang & X. Zhang & J. Li. "Reviews of power systems and environmental energy conversion for unmanned underwater vehicles". In: *Renewable and Sustainable Energy Reviews* 16 (2012), pp. 1958–1970. DOI: https://doi.org/10.1016/j.jrser.2012.12.016.

[13] Oistein Hasvold & N.J. Storkersen & S. Forsbeth & T. Lian. "Power sources for autonomous underwater vehicles". In: *Journal of Power Sources* 162 (2006), pp. 935–942. DOI: https://doi.org/10.1016/j.jpowsour.2005.07.021.

[14] Jay Pukrushpan. “Modeling and Control of Fuel Cell Systems and Fuel Processors”. In: (Jan. 2003).

[15] D. Yang & M. Steinbugler & R. Sawyer & L. Van Dine & C. Reiser. “Procedure for starting up a fuel cell system having an anode exhaust recycle loop”. 20030129462. 2003.

[16] D. Yang & R. Sawyer & C. Reiser. “Procedure for shutting down a fuel cell system using air purge”. 20020076583. 2002.

[17] Sharon Thomas and Marcia Zalbowitz. *Fuel Cell Green Power*. Technical report, Los Alamos National Laboratory.

[18] Q. Ding & K. Zhu & C. Yang & X. Chen & Z. Wan & X.Wang. “Performance investigation of proton exchange membrane fuel cells with curved membrane electrode assemblies caused by pressure differences between cathode and anode”. In: *Inernational Journal of Hydrogen Energy* 46.75 (2021), pp. 37393–37405. DOI: https://doi.org/10.1016/j.ijhydene.2021.09.005.

[19] M. Bargal & M. Abdelkareem & Q. Taon & J. Li & J. Shi & Y.Wang. “Liquid cooling techniques in proton exchange membrane fuel cell stacks: A detailed survey”. In: *Alexandria Engineering Journal* 59.2 (2020), pp. 635–655. DOI: 10.1016/j.aej.2020.02.005.

[20] Erik Zakrisson. “The Effect of Start/Stop Strategy on PEM Fuel Cell Degradation Characteristics”. In: (2011).